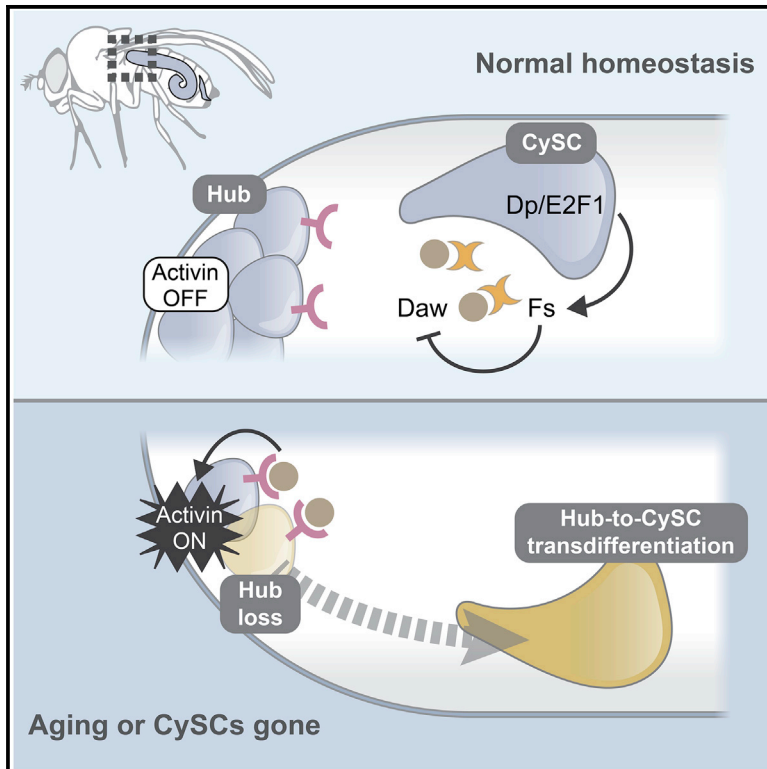


# Developmental Cell

## Proliferative stem cells maintain quiescence of their niche by secreting the Activin inhibitor Follistatin

### Graphical abstract



### Authors

Salvador C. Herrera,  
Diego Sainz de la Maza,  
Lydia Grmai, ..., Michael O'Connor,  
Marc Amoyel, Erika A. Bach

### Correspondence

marc.amoyel@ucl.ac.uk (M.A.),  
erika.bach@nyu.edu (E.A.B.)

### In brief

How stem cells support niches remains largely unknown. Herrera et al. show that testicular stem cells maintain niche quiescence by secreting Follistatin, an Activin antagonist. Loss of Follistatin in stem cells or gain of Activin signaling in niche cells causes niche-to-stem-cell transdifferentiation, and this process underlies niche decay during aging.

### Highlights

- Dp/E2f1 is required in stem cells to non-autonomously maintain niche quiescence
- Dp/E2f1 promotes niche quiescence through Fs, an Activin antagonist
- Activin signaling in niche cells causes transdifferentiation into functional stem cells
- Fs in stem cells regulates the physiological decay of the niche with age

## Article

# Proliferative stem cells maintain quiescence of their niche by secreting the Activin inhibitor Follistatin

Salvador C. Herrera,<sup>1,2</sup> Diego Sainz de la Maza,<sup>3</sup> Lydia Grmai,<sup>1,6</sup> Shally Margolis,<sup>1,7</sup> Rebecca Plessel,<sup>1</sup> Michael Burel,<sup>1</sup> Michael O'Connor,<sup>4</sup> Marc Amoyel,<sup>3,5,\*</sup> and Erika A. Bach<sup>1,5,8,\*</sup>

<sup>1</sup>Biochemistry and Molecular Pharmacology, NYU Grossman School of Medicine, New York, NY 10016, USA

<sup>2</sup>Centro Andaluz de Biología del Desarrollo, CSIC/Universidad Pablo de Olavide/JA, Carretera de Utrera km 1, 41013 Sevilla, Spain

<sup>3</sup>Department of Cell and Developmental Biology, University College London, Gower Street, London WC1E 6BT, UK

<sup>4</sup>Department of Genetics, Cell Biology and Development, University of Minnesota, Minneapolis, MN 55455, USA

<sup>5</sup>Senior author

<sup>6</sup>Present address: Department of Biology, Johns Hopkins University, Baltimore, MD 21218, USA

<sup>7</sup>Present address: Molecular and Cellular Biology, University of California, Berkeley, Berkeley, CA 94720-3200, USA

<sup>8</sup>Lead contact

\*Correspondence: [marc.amoyel@ucl.ac.uk](mailto:marc.amoyel@ucl.ac.uk) (M.A.), [erika.bach@nyu.edu](mailto:erika.bach@nyu.edu) (E.A.B.)

<https://doi.org/10.1016/j.devcel.2021.07.010>

## SUMMARY

Aging causes stem cell dysfunction as a result of extrinsic and intrinsic changes. Decreased function of the stem cell niche is an important contributor to this dysfunction. We use the *Drosophila* testis to investigate what factors maintain niche cells. The testis niche comprises quiescent “hub” cells and supports two mitotic stem cell pools: germline stem cells and somatic cyst stem cells (CySCs). We identify the cell-cycle-responsive Dp/E2f1 transcription factor as a crucial non-autonomous regulator required in CySCs to maintain hub cell quiescence. Dp/E2f1 inhibits local Activin ligands through production of the Activin antagonist Follistatin (Fs). Inactivation of Dp/E2f1 or Fs in CySCs or promoting Activin receptor signaling in hub cells causes transdifferentiation of hub cells into fully functional CySCs. This Activin-dependent communication between CySCs and hub regulates the physiological decay of the niche with age and demonstrates that hub cell quiescence results from signals from surrounding stem cells.

## INTRODUCTION

The niche creates a distinct microenvironment for stem cells and secretes short range self-renewal cues that promote “stemness” in the resident population (Morrison and Spradling, 2008). Decreased stem cell function with age can at least in part be attributed to both decreased niche function and niche cell numbers (Oh et al., 2014). These observations raise the question of what factors maintain niche cells. The *Drosophila* testis provides an ideal system to address this important issue. The testis niche comprises approximately twelve quiescent somatic hub cells that support two mitotic stem cell pools: germline stem cells (GSCs) that ultimately produce sperm and somatic cyst stem cells (CySCs) that support GSCs and produce somatic support cells. The hub and CySCs share a common lineage during development: somatic cells are initially all equivalent somatic gonadal precursors, but during embryonic stages, a subset of these are specified to become hub cells (Okegbe and DiNardo, 2011; Dinardo et al., 2011; Le Bras and Van Doren, 2006; Anillo et al., 2019; Kitadate and Kobayashi, 2010). The remaining somatic precursors become CySCs and their offspring, cyst cells. Intriguingly, despite their common origin, CySCs are the only somatic cells in the testis to proliferate, and both hub and cyst cells

are post-mitotic. Since they cease proliferating, hub cells need to be maintained during adulthood; previous work has identified several factors that act autonomously within the hub to maintain quiescence or survival (Hétié et al., 2014; Voog et al., 2014; Resende et al., 2013; Greenspan and Matunis, 2018). These include the transcription factor Escargot (Esg), as well as the cell-cycle-inhibitor retinoblastoma homolog, Rbf. Most intriguingly, prior work has shown that genetic ablation of all CySCs causes hub cells to exit quiescence and transdifferentiate into CySCs, suggesting the existence of unidentified CySC-derived factors that non-autonomously maintain hub cells (Hétié et al., 2014). Finally, during normal aging, the ability of the hub to support stem cells declines. This is due both to a reduction in hub cell numbers (Sreejith et al., 2019; Wallenfang et al., 2006; Lee et al., 2016), as well as lower production of self-renewal ligands to support surrounding stem cells (Toledano et al., 2012; Boyle et al., 2007). Yet how the mechanisms maintaining hub cell quiescence are affected during aging is still unknown.

Here, we identify how CySCs maintain hub cell quiescence. We find that hub cells are lost following depletion of the transcription factor that regulates S-phase gene expression, which is a complex of the activator E2f, called E2f1 in *Drosophila*, and the sole dimerization partner homolog, Dp, in CySCs. This

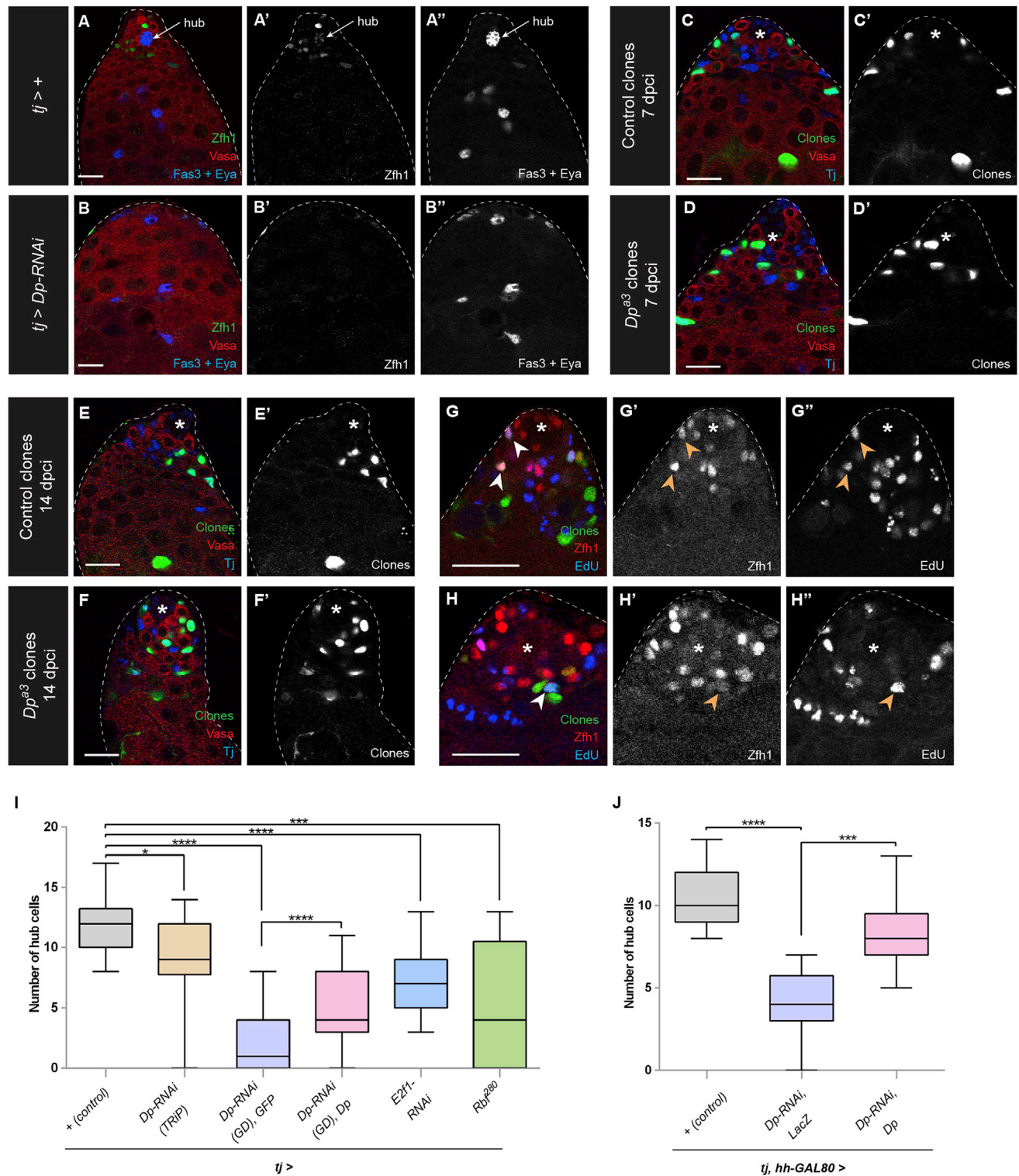


**Figure 1. Dp/E2f1 is required in CySCs to maintain hub cells**

(A and B) A control *tj-GAL4* (labeled *tj*>+) adult testis with hub cells (A, arrow) surrounded by both GSCs and CySCs. A *tj*>*Dp-RNAi* (B) adult testis lacking CySCs, GSCs, and hub cells. Both testes were isolated after 10 days at 29°C to induce maximal GAL4 activity. Zfh1 (green) labels CySCs, Vasa (red) marks the germline, Fas3 (blue) marks the hub cell membranes, and Eya (blue) labels the nucleus of differentiating cyst cells.

(C–H) GFP-positive *FRT<sup>42D</sup>* control clones (C, E, and G) or *FRT<sup>42D</sup>* *Dp<sup>a3</sup>* mutant clones (D, F, and H). Both types of CySC clones can be recovered at 7 days post clone induction (dpi) (C and D) and 14 dpi (E and F) and both incorporate EdU (blue, G and H), indicating that they can undergo S phase. Clones are marked by GFP (green), Vasa (red, C–F) marks the germline, and Tj (blue, C–F) marks CySCs and early cyst cells. Zfh1 (blue, G and H) marks CySCs.

(legend continued on next page)

signaling between cycling CySCs and the hub is mediated through production of Follistatin (Fs), an antagonist of Activin signaling. Finally, we show that Activin autonomously promotes hub cells to transdifferentiate into CySCs, leading to hub cell loss, and that increased activity of this pathway is responsible for age-dependent loss of hub cells.

## RESULTS

### Dp/E2f1 functions in CySCs to non-autonomously maintain hub cells

Our prior work focused on how cell-cycle progression in CySCs, the only mitotic somatic cells in the testis, influenced cell fate (Amoyel et al., 2014). Here, we focused on the transcription factor that regulates S-phase gene expression, which is a complex of E2f1 and Dp, and which we previously reported to be active in CySCs (Amoyel et al., 2014). Knockdown of *Dp* by RNAi using the cyst lineage driver *traffic jam (tj)-GAL4* resulted in a complete loss of CySCs, as identified by *Zfh1* expression, and only *Eya*-positive differentiated cyst cells were visible (Leatherman and Dinardo, 2008; Fabrizio et al., 2003) (Figures 1A and 1B). In most cases (12/20), testes with somatic *Dp* depletion lacked the entire stem and early-differentiated cell compartment for both somatic and germ lineages and contained only spermatocytes or spermatid fibers. This suggested that *Dp* was required for CySC self-renewal and that its loss resulted in ectopic and premature differentiation. To confirm this, we used mitotic recombination to generate clones mutant for *Dp*. Surprisingly, *Dp*-mutant CySC clones, which we identified as *Tj*-positive cells adjacent to the hub, were recovered at similar rates to control clones, both 7 days post clone induction (dpci) and 14 dpci (Figures 1C–1F, S1A, and S1B), indicating that they had no autonomous self-renewal defect. We confirmed this result using an independent *Dp* null allele and used an antibody against Dp to verify that the mutant clones lacked Dp protein (Figures S1A–S1C). Similarly, CySC clones expressing the same *Dp*-RNAi as in Figure 1B were also recovered at 7 dpci (Figure S1D). *Dp* null mutant clones resulting from single-clonal-induction events contained many cells, indicating that they had proliferated over the course of the experiment (Figure 1D). Indeed, *Dp*-mutant CySCs were found to incorporate the nucleotide analog 5-ethynyl-2'-deoxyuridine (EdU), demonstrating that cells lacking *Dp* could undergo DNA replication (Figures 1G, 1H, S1A, and S1E, arrowheads). Consistently, we recovered clones mutant for *E2f1*, the sole activator E2f in *Drosophila*, at similar rates to control clones at 7 dpci (Figures S1F and S1G). Although surprising, this result concurs with recent work showing that *Dp* is dispensable for most larval proliferation in *Drosophila* and that viable adults lacking Dp in all but muscle tissues can be obtained (Zappia and Frolov, 2016). Similarly in mouse, proliferation still occurs in the absence of all activating E2fs (Chen et al., 2009).

The fact that *Dp* was not required autonomously for CySC self-renewal, but its depletion in all CySCs led to loss of the entire stem cell population suggested that *Dp* may be required in a non-autonomous manner to maintain CySCs. Indeed, we noticed that in addition to loss of CySCs, hub cells were also absent in testes in which *Dp* was knocked down with *tj-GAL4* (Figures 1A, 1B, and 1I). Whereas in controls the hub is composed of  $11.8 \pm 0.5$  cells, when *Dp* was knocked down in the cyst lineage, there were many fewer cells ( $2.1 \pm 0.4$ ). To verify this observation, we used the markers *upd-LacZ* and *hh-LacZ* to label hub cells and found a reduction of labeled cells in the *Dp* knockdown and, in many cases, no cells expressing these markers (Tulina and Matunis, 2001; Forbes et al., 1996; Amoyel et al., 2013) (Figures S2A–S2D). To confirm that this phenotype was due to loss of *Dp* and not an off-target effect of the RNAi, we used three approaches: first, we expressed full-length *Dp* together with *Dp*-RNAi and observed a partial rescue of hub cell numbers compared with co-expressing GFP as a titration control (Figure 1I, compare purple with pink bar); second, we used an independent RNAi line targeting *Dp*, which gave a similar, albeit weaker, loss of hub cells (Figure 1I, compare brown with gray bar); third, we inactivated the *Dp/E2f1* transcription factor by knocking down *E2f1* or overexpressing a constitutively active form of the *Dp/E2f1* inhibitor Rbf, called Rbf<sup>280</sup>, which recapitulated the loss of hub cells observed in *Dp* knockdowns in both cases (Figure 1I, compare blue and green bars with gray bar).

We then ruled out the possibility of hub loss being due to a developmental defect of the *Dp*-RNAi by using a temperature-sensitive form of GAL80 (GAL80<sup>TS</sup>) to only induce transgene expression in adult stages (McGuire et al., 2004). We analyzed flies at eclosion (0 days) after raising them at the permissive temperature for GAL80<sup>TS</sup> (18°C) and observed no significant differences in hub cell numbers between control flies expressing *tj-GAL4* and GAL80<sup>TS</sup>, referred to as *tj*<sup>TS</sup>, and flies also carrying *Dp* or *E2f* RNAi transgenes (Figure S2E). After shifting to the restrictive temperature, we observed no significant change in hub cells in control *tj*<sup>TS</sup> flies over 10 days, although we see a slight but not significant decrease in 20-day-old flies. By contrast, *Dp* knockdown, *E2f1* knockdown, or Rbf<sup>280</sup> overexpression in CySCs led to a progressive loss of hub cells and an almost complete loss ( $0.03 \pm 0.03$  in the *Dp* knock down) by 20 days of adulthood (Figure S2E and Table S1). Altogether, these results indicate that the hub cell loss observed in *Dp* knockdowns is due to a progressive defect in maintenance of hub cells, not in their establishment.

We sought to establish that *Dp/E2f1* function was indeed required, specifically in CySCs, to maintain hub cells non-autonomously. Since *tj-GAL4* is occasionally expressed in hub cells (Fairchild et al., 2016), we generated a strain expressing GAL80 under the control of the endogenous *hh* locus, which is

(I) Graph showing the average number of hub cells after 10 days in 29°C using *tj-GAL4* in control (+, gray bar,  $n = 18$ ), *Dp*-RNAi (brown and purple bars,  $n = 14$  and  $n = 31$ , respectively), *Dp* depletion plus exogenous *Dp* (pink bar,  $n = 15$ ), *E2f1* depletion (blue bar,  $n = 17$ ), and overexpression of Rbf<sup>280</sup> (green bar,  $n = 12$ ).

(I and J) Graphs showing the average number of hub cells after 10 days in 29°C using *tj-GAL4* and *hh-GAL80*, which inhibits GAL4 activity in the hub, limiting expression of UAS-dependent constructs to CySCs in control (+, gray bar,  $n = 27$ ), *Dp*-RNAi (purple bar,  $n = 8$ ), and *Dp* depletion plus exogenous *Dp* (pink bar,  $n = 33$ ).

An asterisk marks the hub.

Error bars represent the data range. \*\*\*\* $p < 0.0001$ ; \*\*\* $p < 0.001$ ; \* $p < 0.05$  as assessed by Student's *t* test.

See also Tables S1 and S2; Figures S1 and S2. Scale bar, 20  $\mu$ m.

expressed exclusively in hub cells (see [STAR Methods](#)) (Amoyel et al., 2013; Michel et al., 2012). Importantly, knockdown of *Dp* using *tj-GAL4* led to significant loss of hub cells in a *hh-GAL80* background ( $4.0 \pm 0.8$  hub cells in *Dp*-RNAi versus  $10.6 \pm 0.3$  in control, [Figure 1J](#), purple bar). As expected, hub cell loss was suppressed by co-expressing *Dp* in non-hub somatic cells ( $8.4 \pm 0.3$  hub cells versus  $4.0 \pm 0.8$  in controls expressing LacZ as a titration control,  $n = 33$  and  $8$ , respectively,  $p < 0.001$ , [Figure 1J](#), pink bar). Finally, to rule out any possibility of ectopic hub expression of the RNAi, we used alternative GAL4 lines, which drive expression in CySCs and cyst cells and which were previously shown to have sporadic or negligible expression in hub cells: *eyaA3-GAL4* (Fairchild et al., 2016), *fringe (fng)-GAL4* (Dinardo et al., 2011), and *C587-GAL4* (Fairchild et al., 2016; Hétié et al., 2014). Knockdown of *Dp* using all three drivers resulted in a loss of hub cells ([Figure S2F](#)). In the case of *fng-GAL4*, we used *GAL80<sup>TS</sup>* to show progressive hub cell loss in adult flies when *Dp* or *E2f1* were knocked down ([Figure S2F](#) and [Table S1](#)). In sum, our results indicate that activity of the *Dp/E2f1* transcription factor is dispensable within individual CySCs for cell-cycle progression but that its loss in all adult CySCs results in a progressive and non-autonomous loss of hub cells. These observations suggest a model in which *Dp/E2f1* activity in CySCs causes them to signal to hub cells to promote their maintenance in adult testes.

#### Dp/E2f1 regulates follistatin expression to maintain the hub non-autonomously

To determine the signals downstream of *Dp/E2f1* that acted on the hub non-autonomously, we performed an RNAi screen. We used *tj-GAL4* to deplete from CySCs secreted factors that are enriched in testicular stem cells and then assessed hub cell number (Terry et al., 2006; Kurusu et al., 2008) ([Figure S3A](#)). Knockdown of *Fs*, encoding a conserved repressor of TGF $\beta$ /Activin ligands ([Figure 2A](#)) (Pentek et al., 2009), recapitulated the phenotypes observed with *Dp* or *E2f1* knockdown. After 14 days of RNAi expression, *tj>Fs-RNAi* testes contained  $1.1 \pm 0.3$  hub cells, whereas control *tj>LacZ* testes had  $9.7 \pm 0.5$  hub cells ([Figures 2B–2D](#)). Frequently, *tj>Fs-RNAi* testes contained 0 hub cells. In these testes, both stem cell populations were lost, and we frequently observed only differentiated spermatids, indicating that all the more undifferentiated cell types had been lost to ectopic differentiation ([Figures S3B](#) and [S3C](#)). The specificity of the *Fs*-RNAi transgene was confirmed by qRT-PCR analysis showing a significant decrease in *Fs* transcripts in *tj>Fs-RNAi* testes ([Figures S3D](#) and [S3E](#)) and by a significant rescue of hub cells when full-length *Fs* was concomitantly overexpressed with *Fs-RNAi* ([Figure 2D](#)). Overexpression of wild-type *Fs* alone using *tj-GAL4* did not affect the number of hub cells ([Figure 2D](#)). No phenotype was observed when *Fs* was depleted from the germline using *nanos (nos)-GAL4* ([Figure S3F](#)).

To confirm these results, we generated a *Fs<sup>null</sup>* allele lacking the sequence spanning coding exons 1 and 4 ([Figure S3D](#), see [STAR Methods](#)). The deletion was confirmed by sequencing and by RT-qPCR ([Figure S3E](#)). *Fs<sup>null</sup>* flies were adult viable and showed progressive hub cell loss with age: from  $9.4 \pm 0.9$  hub cells in 0-day-old adult flies to  $2.2 \pm 0.6$  hub cells in 28-day-old flies ([Figures 2E](#) and [S3G](#)). Hub cell loss in the *Fs<sup>null</sup>* mutant was significantly rescued by overexpressing wild-type *Fs* in either somatic cells

(*fng-GAL4*) or hub cells (*upd<sup>TS</sup>-GAL4*) ([Figures S3H](#) and [S3I](#)). Furthermore, we observed similar hub cell loss in testes from trans-heterozygous combinations of other *Fs* alleles ([Figure S3J](#)). As expected, 28-day-old *Fs<sup>null</sup>* males were significantly less fertile than age-matched control flies ([Figure 2F](#)). Using a *Fs-GAL4* transcriptional reporter, we found that *Fs* was expressed in hub cells, CySCs and early somatic cells ([Figure 2G](#)).

Given the remarkable similarity in the non-autonomous hub cell phenotypes observed upon *Dp/E2f1* or *Fs* loss in CySCs, we asked whether *Fs* functioned downstream of the *Dp/E2f1* complex in CySCs. To test this, we examined expression of the *Fs-GAL4* transcriptional reporter in control testes or in testes somatically depleted for *Dp*. *Fs* transcription in the somatic lineage, as assessed by *UAS-GFP* expression, was significantly reduced when *Dp* was depleted compared with controls ([Figures 2G–2I](#)). We observed a similar reduction in the levels of an *Fs-GFP* protein trap upon *E2f1* knockdown ([Figures S4A–S4C](#)). We reasoned that if *Dp/E2f1* activity in CySCs non-autonomously maintained the hub by inducing *Fs* expression, then hub cell loss caused by *Dp* depletion should be prevented when *Fs* was concomitantly supplied. Indeed, exogenous *Fs* completely rescued hub cell loss compared with *Dp-RNAi* alone ([Figure 2J](#); [Table S1](#)). Thus, *Fs* mediates the non-autonomous effects of *Dp/E2f1* on hub cell maintenance.

#### Activin signaling triggers hub-to-CySC transdifferentiation

Since *Fs* is an extracellular antagonist of Activin ligands, we hypothesized that sustained autonomous activation of the Activin pathway within hub cells would have a similar effect on hub cell maintenance. In *Drosophila*, three Activin ligands (Dawdle [Daw], Activin $\beta$  [Act $\beta$ ], and Myoglianin [Myo]) stimulate the type I Activin receptor Baboon (Babo) (Upadhyay et al., 2017). This results in the activation of transcription factor Smox, the SMAD3 homolog, which then alters target gene transcription. *Fs* binds to Activin ligands and prevents them from binding to and activating Babo ([Figure 2A](#)).

First, we determined that hub cells can indeed respond to Activin ligands, by examining the distribution of the receptor. A protein trap for Babo was present at the surface of many cells in the testis, and importantly, was found decorating the membrane of Fas3-positive hub cells ([Figure 3A](#)). Next, we tested what effect Activin pathway signaling had within hub cells. We used *upd-GAL4* and *GAL80<sup>TS</sup>* (termed *upd<sup>TS</sup>*) to overexpress a constitutively active form of Babo (Babo<sup>QD</sup>) (Brummel et al., 1999) in hub cells and assessed hub cell number at 0, 7, 14, 21, and 28 days of adulthood. Freshly eclosed flies that were raised at the permissive temperature for *GAL80<sup>TS</sup>* had no significant differences in hub cell numbers, whether or not they carried the *UAS-babo<sup>QD</sup>* transgene ([Figure 3B](#)). After shifting to the restrictive temperature, autonomous activation of the Activin pathway (*upd<sup>TS</sup>>babo<sup>QD</sup>*) in hub cells induced their progressive and complete loss by 28 days, whereas controls showed a modest decrease in hub cell number over this period ([Figures 3B](#) and [3C](#)). We then asked what the fate of lost hub cells with ectopic Activin signaling could be and hypothesized that, since hub cells have the potential, under certain experimental conditions, to transdifferentiate into CySCs (Hétié et al., 2014; Voog et al., 2014; Greenspan and Matunis, 2018), Activin signaling may induce this identity switch. To test this

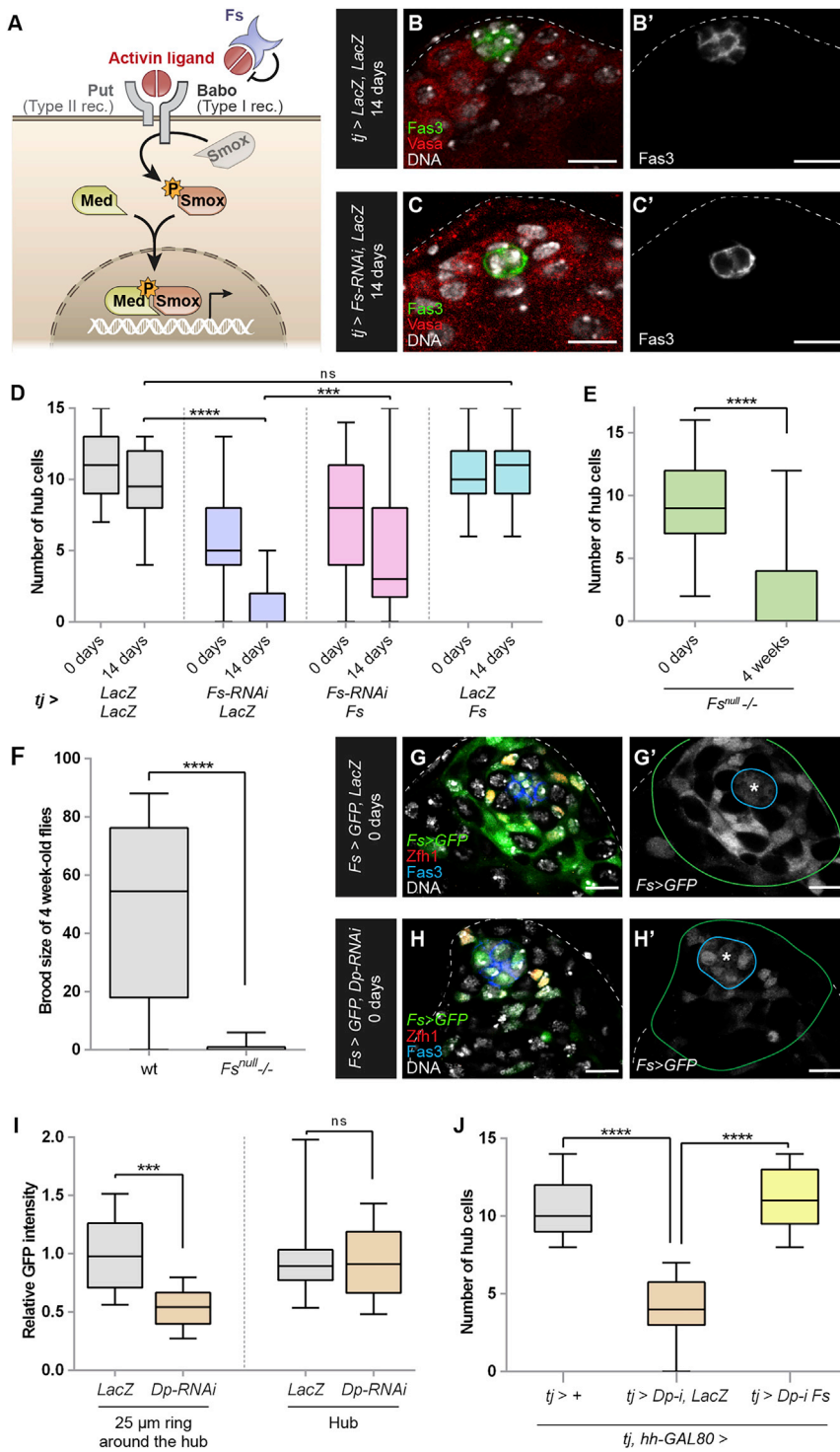


**Figure 2. Follistatin acts downstream of Dp/E2f1 in CySCs to maintain hub cells**

(A) Model of the Activin pathway. Fs (purple) inhibits Activin ligands (red) binding to Activin receptors, Baboon (Babo, type I receptor) and Punt (Put, type II receptor). Receptor activation causes phosphorylation (orange P star) of the SMAD3 homolog Smox (inactive Smox is gray; active Smox is brown). Active Smox associates with the Co-SMAD Medea (Med, yellow) at regulatory sites of target genes to alter transcription.

(B and C) A control *tj-GAL4* (labeled *tj>LacZ, LacZ*) adult testis has a normal number of hub cells (B), whereas a *tj>Fs-RNAi, LacZ* (C) adult testis has only 2 hub cells. Both testes were isolated after 14 days at 29°C to induce maximal GAL4 activity. Fas3 (green) labels hub cells, Vasa (red) marks germ cells, and DNA marked by DAPI is white.

(D) Graph showing the average number of hub cells at 0 and 14 days at 29°C in *tj>LacZ, LacZ* (gray bars, n = 49 and n = 22, respectively), *tj>Fs-RNAi, LacZ* (purple bars, n = 32 and n = 28, respectively), *tj>Fs-RNAi, UAS-Fs* (pink bars, n = 31 and n = 34, respectively), or *tj>LacZ, UAS-Fs* (blue bars, n = 37 and n = 31, respectively). See Table S1 for n values. (E) Graph showing the average number of hub cells at 0 days and 4 weeks in *Fs<sup>null</sup>/-* mutant (n = 18 and n = 31, respectively).

(F) Graph showing the fertility (brood size) at 4 weeks in a control and *Fs<sup>null</sup>/-* mutant (n = 50 in both cases).

(G and H) Expression at 0 days of adulthood of *Fs-GAL4* in a control testis (*Fs>GFP, LacZ*) or a testis in which Dp was depleted throughout development (*Fs>GFP, Dp-RNAi*). *Fs-GAL4* is expressed strongly in CySCs and early cyst cells and weakly in hub cells (G) but its expression is substantially reduced when Dp is depleted (H). GFP (green) labels *Fs-GAL4*-expressing cells, Zfh1 (red) marks CySCs, Fas3 (blue) marks hub cells, and DNA marked by DAPI is white. Blue line surrounds hub cells and green line marks 25 μM away from the hub.

(I) Graph of relative GFP intensity in *Fs>GFP, LacZ* (gray bars, n = 13) or *Fs>GFP, Dp-RNAi* testes (labeled *Dp-RNAi*, brown bars, n = 13) in CySCs and early cyst cells (i.e., area between blue and green lines in (G and H) (labeled “25 μM ring around the hub”) and in hub cells (i.e., the area within the blue line, labeled “Hub”).

(J) Graph of the number of hub cells in testes from control *tj-GAL4, hh-GAL80* males (gray bar, labeled “*tj>+*,” n = 27) or these males expressing *Dp-RNAi* and *LacZ* (brown bar, n = 8) or expressing *Dp-RNAi* and *UAS-Fs* (yellow bar, n = 17). *UAS-Fs* significantly rescues hub cell number compared with *Dp-RNAi* alone.

Error bars represent the data range. \*\*\*\* p < 0.0001; \*\*\* p < 0.001. ns = not significant as assessed by Student’s t test.

See also Tables S1 and S2; Figures S3 and S4. Scale bar, 10 μM.

possibility, we permanently labeled the hub cell lineage with GFP (see STAR Methods, Figures 3D–3F). In testes where *babo<sup>QD</sup>* was overexpressed using *upd<sup>TS</sup>*, 67% of CySCs and early differentiating cyst cells (labeled by Zfh1) were GFP-positive after

14 days, indicating that they originated from hub cell transdifferentiation (Figures 3E and 3F). In contrast, in control testes, only 9% of Zfh1-positive CySCs and their immediate daughter cells were GFP-positive (p < 0.0001) (Figures 3D and 3F).

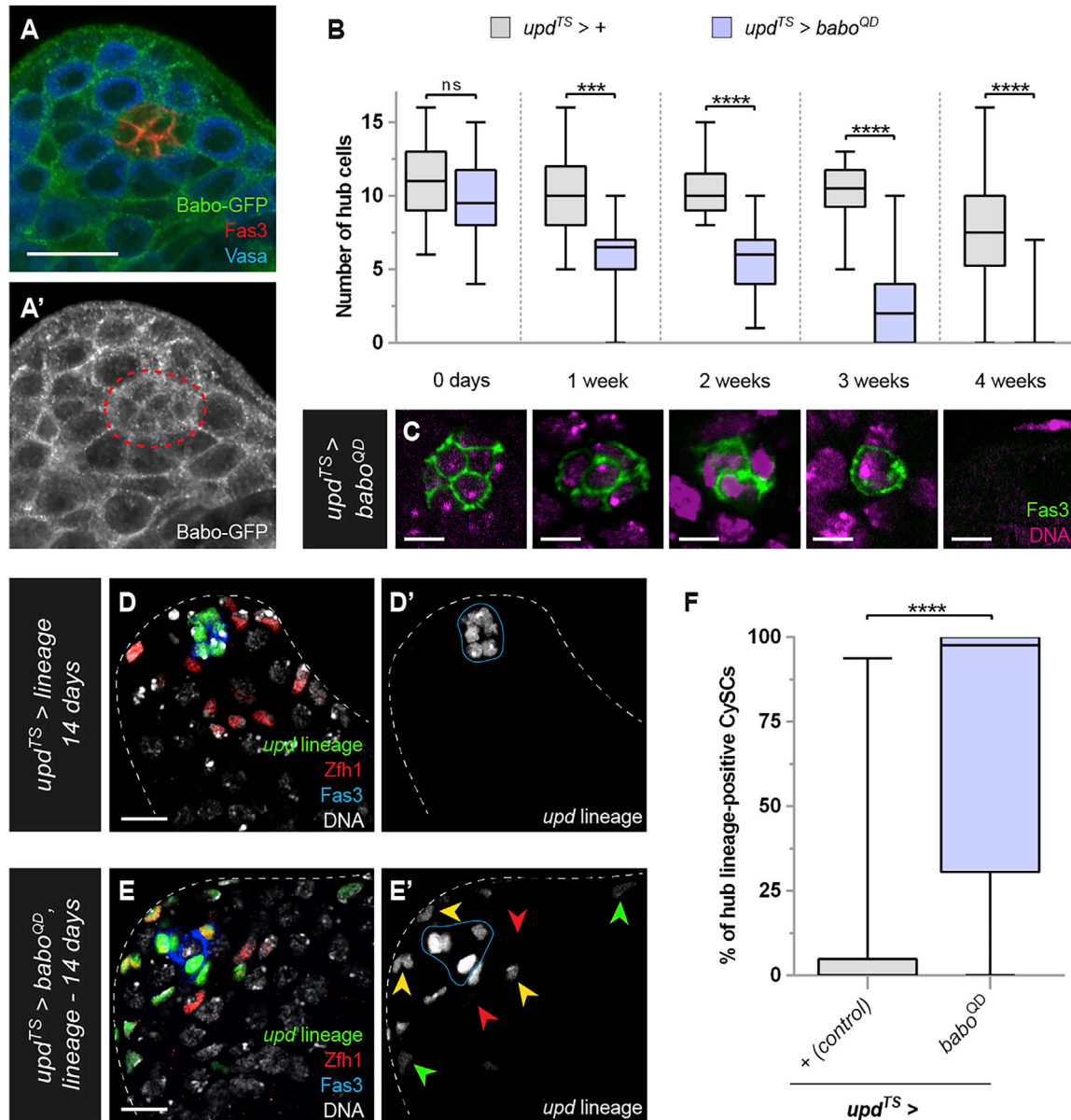


**Figure 3. Autonomous Activin signaling disrupts hub cell quiescence**

(A) Expression of Babo-GFP fusion protein (green, single channel in A') is detected in the testis apex. In particular, Babo-GFP expression is visible in hub cells (labeled with Fas3, red), outlined with a red dashed line in (A'). Vasa (blue) labels the germline.

(B) Graph showing the number of hub cells in control testes ( $upd^{TS} > +$ , gray bars,  $n = 23$  for 0 days,  $n = 15$  for 1 week,  $n = 13$  for 2 weeks,  $n = 8$  for 3 weeks,  $n = 84$  for 4 weeks) or those with sustained Activin signaling in hub cells ( $upd^{TS} > babo^{OD}$ , purple bars,  $n = 16$  for 0 days,  $n = 16$  for 1 week,  $n = 28$  for 2 weeks,  $n = 35$  for 3 weeks,  $n = 30$  for 4 weeks) at the indicated time points. Note the progressive loss of hub cells in  $upd^{TS} > babo^{OD}$ .

(C) Confocal sections of  $upd^{TS} > babo^{OD}$  testes at the indicated time points. Fas3 (green) marks hub cells and TO-PRO (magenta) marks DNA.

(D and E) Lineage tracing hub cells in control  $upd^{TS} > +$  (D) and  $upd^{TS} > babo^{OD}$  testes (E). Note in (E) the presence of hub-lineage-positive (green) cells outside of the niche that express the CySC marker Zfh1 (red). Fas3 (blue) marks hub cells and TO-PRO (DNA) is white. In (E'), yellow and red arrowheads indicate hub-lineage-positive CySCs and hub-lineage-negative CySCs, respectively, and the green arrowheads indicate differentiating cyst cells descended from a hub-lineage CySC. Blue lines in (C and D) indicate Fas3-positive hub cells.

(F) Graph indicating the percentage of CySCs positive for hub lineage in  $upd^{TS} > +$  (gray bar,  $n = 34$ ) and  $upd^{TS} > babo^{OD}$  (purple bar,  $n = 26$ ) testes.

Error bars represent the data range. \*\*\*\* $p < 0.0001$ ; \*\*\* $p < 0.001$ . ns, not significant as assessed by Student's *t* test.

See also [Tables S1](#) and [S2](#).

Scale bar, 5  $\mu$ M in (C) and 10  $\mu$ M in all other panels.

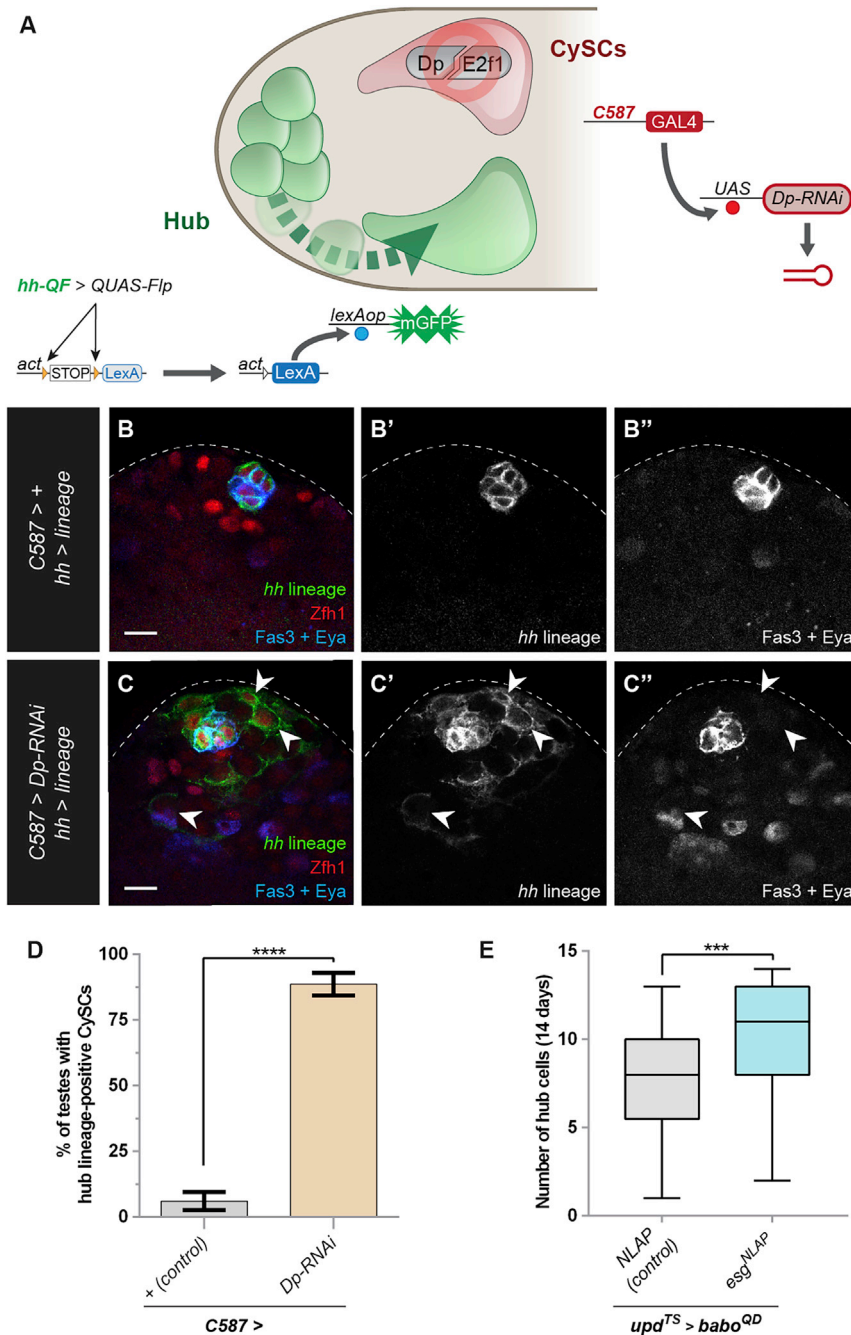


**Figure 4. CySC depletion of *Dp* results in non-autonomous hub-to-CySC transdifferentiation**

(A) Model indicating experimental design to deplete *Dp* from CySCs while concomitantly tracing hub cells using independent binary expression systems. To trace the lineage of hub cells, we used *hh-QF*, which is expressed only in hub cells, to induce *QUAS-FLP*. In turn, FLP recombines *FRT* sites in the *act>STOP>LexA* transgene. This leads to the production of LexA. Then LexA induces expression of *lexAop-GFP*, hereby exclusively labeling hub cells and their lineage with membrane GFP. In the same animal, *C587-GAL4* drives expression of a *Dp-RNAi* transgene, which depletes *Dp* from CySCs but not from hub cells.

(B and C) There are GFP-positive cells expressing *Zfh1* (C, arrowheads) outside the cluster of hub cells in a *C587>Dp-RNAi; hh>lineage* testis but not in a control *C587>+; hh>lineage* testis (B). Hub lineage is in green, *Zfh1* (red) labels CySCs, *Fas3* (blue) labels hub cell membranes, and *Eya* (blue) labels the nuclei of differentiating cyst cells.

(D) Graph showing the percentage of testes in which hub-lineage-positive CySCs were present in *C587>+* (control) (gray bar,  $n = 53$ ) or *C587>Dp-RNAi* (brown bar,  $n = 49$ ).

(E) Graph of the number of hub cells in testes in which *babo<sup>OD</sup>* was mis-expressed in hub cells (*upd<sup>TS</sup>>*) with either *escargot (esg-NLAP)*, gray bar,  $n = 41$ ) or the control transgene (*NLAP*, blue bar,  $n = 38$ ).

Error bars represent the data range. \*\*\*\*  $p < 0.0001$ ; \*\*\*  $p < 0.001$  as assessed by Fisher's exact test (D) or Student's *t* test (E).

See also Tables S1 and S2, Figure S5. Scale bar, 10  $\mu$ M.

Since autonomous activation of Activin signaling resulted in hub-to-CySC transdifferentiation, we asked whether knocking down *Dp* in CySCs also resulted in ectopic transdifferentiation of hub cells, leading to their eventual complete loss. We designed a strategy to trace the hub cell lineage, while simultaneously knocking down *Dp* in CySCs by employing orthogonal binary expression strategies (Figures 4A and S5A, see STAR Methods). In control genotypes, where *Dp* was not depleted in CySCs, hub-lineage-derived cells were detected infrequently outside the hub, in 6%–14% of testes (Figures 4B, 4D, S5B, S5C, and S5E) consistent with prior results (Voog et al., 2014). By contrast, hub-lineage-pos-

itive CySCs were detected in 87%–89% of testes when *Dp* was depleted from all CySCs, a significant increase compared with controls (Figures 4C, 4D, S5B, S5D, S5F, and S5G). These cells lacked the hub cell marker *Fas3* but expressed high levels of the CySC marker *Zfh1*, suggesting that they had adopted CySC identity (Leatherman and Dinardo, 2008) (Figures 4C, S5D, S5F, and S5G). Importantly, hub-lineage-expressing cells could incorporate the S-phase marker EdU (Figures S5E and S5F), a marker of CySC identity. Additionally, lineage-positive cells many cell diameters away from the niche presented long membrane extensions and expressed the differentiation marker *Eya* (Figures 4C and S5G), suggesting that transdifferentiated hub cells are functional CySCs, capable of proliferating and differentiating. Taken together, our data demonstrate that autonomously increasing Activin signaling in hub cells or non-autonomously depleting *Dp* from CySCs lead to transdifferentiation of hub cells into CySCs and that these new hub-derived CySCs display all the hallmarks of stem cell behavior, namely self-renewal and differentiation.

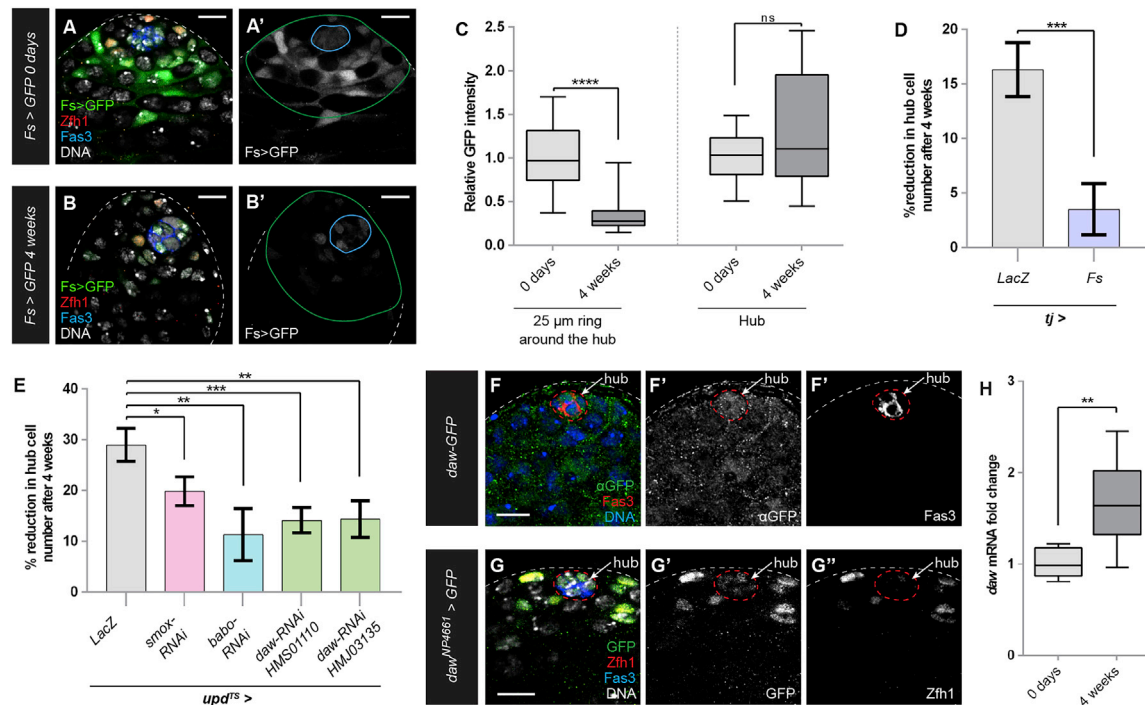


**Figure 5. Increased Activin signaling is responsible for the decline of hub cell numbers during normal aging**

(A–C) Expression at 0 days (A) and 4 weeks (B) of adulthood of *Fs-GAL4, UAS-GFP* in a control testis (*Fs>GFP*). *Fs-GAL4* is expressed strongly in CySCs and early cyst cells and weakly in hub cells (A), and its expression is substantially reduced at 4 weeks of age (B). GFP (green) labels *Fs-GAL4*-expressing cells, Zfh1 (red) marks CySCs, Fas3 (blue) marks hub cells, and DNA labeled with DAPI is white. Blue line surrounds hub cells and green line marks a 25  $\mu$ m ring from the hub. (C) Graph of relative GFP intensity in *Fs>GFP* testes at 0 days (light gray bars, n = 15) or 4 weeks (dark gray bars, n = 17) in CySCs and early cyst cells (i.e., area between blue and green lines in (A) and (B) (labeled “25  $\mu$ m ring around the hub”) and in hub cells (i.e., the area within the blue line, labeled “Hub”). (D) Graph showing the reduction in hub cell number after 4 weeks relative to newly eclosed flies in control *tj>LacZ* (gray bar, n = 49 at 0 days and n = 66 at 4 weeks) and in *tj>Fs* (purple bar, n = 37 at 0 days and n = 42 at 4 weeks). (E) Graph showing the reduction in hub cell number after 4 weeks relative to newly eclosed flies in control *upd>lacZ* (gray bar, n = 45 at 0 days and n = 84 at 4 weeks); *upd>Smox-RNAi* (pink bar, n = 19 at 0 days and n = 47 at 4 weeks); *upd>babo-RNAi* (blue bar, n = 38 at 0 days and n = 26 at 4 weeks); *upd>daw RNAi-HMS01110* (first green bar, n = 33 at 0 days and n = 45 at 4 weeks); *upd>daw RNAi-HMJ03135* (second green bar, n = 29 at 0 days and n = 46 at 4 weeks). (F and G) Expression of *daw* in the testis tip, as detected with a protein trap (F) or enhancer trap (G). Both reporters show weak expression in the hub (marked by Fas3, red in F, blue in G, and indicated with a dotted line). Daw-GFP protein is also detected outside the hub, and the enhancer trap reveals expression in Zfh1-positive CySCs (red, G). (H) Expression of *daw* mRNA increases with age in wild-type testes, as measured by qPCR (n = 8). Error bars represent the data range. \*\*\*\* p < 0.0001; \*\*\* p < 0.001; \*\* p < 0.01; \* p < 0.05; ns = not significant, as assessed by Student’s t test. See also Tables S1 and S2, Figure S6. Scale bar, 10  $\mu$ m.

We sought to define the autonomous relationship between Activin signaling and *Esg*, a Snail family transcriptional repressor required in hub cells to prevent their transdifferentiation into CySCs (Voog et al., 2014). We reasoned that excess *Esg* might be able to counteract the hub cell loss caused by *Babo*<sup>OD</sup>. To test this, we mis-expressed *Esg* while simultaneously inducing Activin signaling and found that sustained *Esg* expression suppressed hub cell loss induced by *Babo*<sup>OD</sup> (Figure 4E). This result indicates that *Esg* functions downstream of or in parallel to Activin signaling in hub cells to maintain hub cell identity.

### The physiological age-dependent loss of hub cells depends on Activin signaling

Our experiments show that loss of *Dp/E2f1* or *Fs* from all CySCs or increased Activin signaling in all hub cells results in loss of hub cells, indicating that CySCs signal to maintain quiescence of hub cells. Since lineage-wide insults are unlikely in normal physiological conditions, we asked what the functional significance of this

CySC-to-hub cell signaling could be. We hypothesized that increased Activin signaling may be responsible for the decrease in the number of hub cells shown to occur during normal aging (Wallenfang et al., 2006; Boyle et al., 2007). Consistent with this, expression of the *Fs>GFP* transcriptional reporter significantly declined in CySCs in testes from 4-week-old flies compared with those from 0-day-old flies (Figures 5A–5C). Importantly, overexpressing *Fs* in CySCs blocked the loss of hub cells in 4-week-old males (Figure 5D). Although age had a significant effect on hub cell number (p = 0.0049), it displayed a strong interaction with genotype (p = 0.0067), indicating that the number of hub cells in *Fs*-overexpressing testes declined significantly less with age. These data implied that in older animals, reduced *Fs* levels could result in increased availability of Activin ligands to induce pathway signaling in hub cells. To test this model, we knocked down the Activin receptor *babo* or the Activin-dependent transcription factor *Smox* in hub cells. In both conditions, the decline in hub cell number was significantly

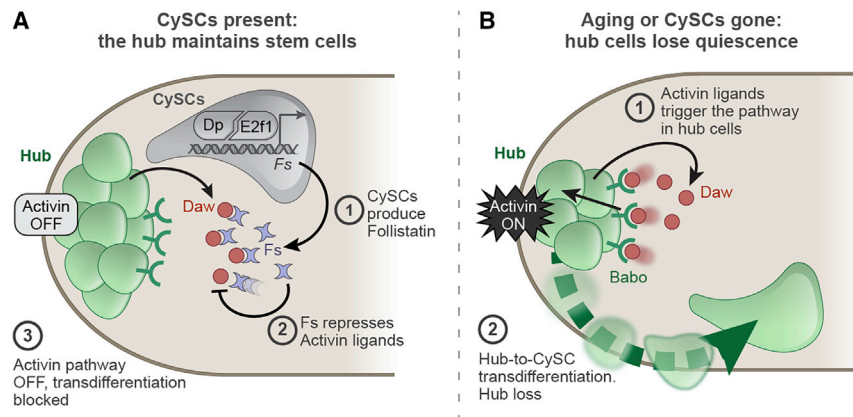


**Figure 6. Model of the communication between CySCs and hub cells that underlies hub cell maintenance**

(A) In a young wild-type testis, hub cells are quiescent. (1) Fs is produced by CySCs downstream of Dp/E2f1 either directly or indirectly. (2) Daw is produced by hub cells and CySCs. Daw is inactivated by Fs and does not activate its receptor Babo on hub cells. (3) In quiescent hub cells, Activin signaling is not activated.

(B) In an old testis or a testis lacking CySCs, (1) Fs expression declines, whereas increased Daw can now activate Babo on hub cells. (2) Activin signaling disrupts hub cell quiescence, leading to hub-to-CySC transdifferentiation.

lower after 4 weeks than in controls (Figure 5E). Finally, we asked which of the Activin ligands was responsible for the age-dependent loss of hub cells. After surveying transcriptional reporters and endogenously tagged Activin ligand lines (Figure S6), we found that only *daw* was expressed in the testis stem cell niche, as both a Daw protein trap (Figure 5F) and two *daw*-GAL4 transcriptional reporters (Figures 5G and S6A) were expressed in hub cells and in CySCs. The transcription of *daw* increased with age, suggesting that it could be partly responsible for the age-related decline of hub cell numbers (Figure 5H). Indeed, knockdown of *daw* in hub cells significantly suppressed their loss in aged testes (Figure 5E). In sum, our data demonstrate that the natural decline in hub cell number during aging is caused, at least in part, by increased Activin signaling in the hub leading to transdifferentiation of hub cells into CySCs.

## DISCUSSION

We uncover a previously unknown aspect of the relationship between stem cells and their niches. Although traditionally thought of as unidirectional and top-down, with niche cells secreting self-renewal factors essential for stem cells, prior work has shown that stem cells can induce their niche, both in normal development, and in malignant situations (Song et al., 2007; Ward et al., 2006; Patel et al., 2015). Here, we show that signals from the stem cells are required continually throughout the lifetime of the animal to maintain their niche. We find that the hub surveils signals from resident stem cells and acts as a reserve pool of stem cells if Activin increases (Figures 6A and 6B). Linking Fs production to Dp/E2f1 activity in CySCs ensures that the hub cells maintain their quiescence when surrounded with proliferating stem cells.

We show that expression of both *Fs* and *daw* in CySCs changes with age and demonstrate that reducing Activin signaling in hub cells significantly ameliorates age-dependent hub cell loss. However, it is interesting that *Fs* expression in hub cells does not decrease with age. Since hub-derived *Fs* can rescue the *Fs*<sup>null</sup> phenotype when overexpressed, suggesting that it is functional, it is likely that hub-derived *Fs* alone is not sufficient to fully inhibit Activin signaling. Similarly, both hub cells and CySCs express *daw*. We show that Daw produced by the hub is relevant to physiological aging and that its knock-

down produces a similar rescue to inhibiting Activin signaling in hub cells through *babo* or *SmoX* knockdown. Thus, it is likely that hub-produced Daw is responsible for all the effects on hub cell numbers with age; however, it would be intriguing to test what the role of Daw produced by CySCs is, both in normal homeostasis and in age-dependent dysfunction.

In mammals, the *Fs* homolog FST is also involved in maintaining fertility via roles in somatic cells (Fullerton et al., 2017), although it has not yet been implicated in regulating the germline stem cell niche. Additionally, similar to our result that Activin signaling can force hub cells to exit quiescence, mammalian TGF $\beta$ /Activin signaling can reverse dormancy in disseminated tumor cells in the bone marrow, leading to tumor growth and metastases (Bragado et al., 2013; Ghajar et al., 2013).

Intriguingly, loss of retinoblastoma, the negative regulator of E2f/Dp transcription, resulted in perturbed interactions between hematopoietic cells and their niche (Walkley et al., 2007). Thus, cells may utilize the E2f/Dp transcription factor in many different contexts to transmit information about their cell-cycle state and allow effective monitoring of stem cells by the niche. Gaining a better understanding of the mechanisms that maintain niches in other stem cell models will enable targeting of the interactions between cancer stem cells and their supportive niches and provide new avenues for therapy (Plaks et al., 2015).

## Limitations of study

Although our study showed no effect of *Dp* loss on CySC function, we cannot rule out that there are defects we failed to detect. Clones mutant for *Dp* persist and proliferate for up to 2 weeks after induction, but they may display defects when aged for longer periods. We showed decreased *Fs* expression upon knockdown of *E2f1* or *Dp*. This could be due to direct or indirect regulation of the *Fs* locus by the E2f1/Dp transcription factor, which would need to be assessed by testing for occupancy of E2f1/Dp at the *Fs* locus. Finally, we show that ectopic Activin signaling promotes hub-to-CySC transdifferentiation and that changes in signaling with age are relevant to physiological hub cell loss. Both *Fs* and *daw* transcript levels change with age, but the mechanisms controlling these changes are unknown. It will be important in future studies to establish what directly regulates expression of these factors and how these regulators change during aging.

## STAR★METHODS

Detailed methods are provided in the online version of this paper and include the following:

- **KEY RESOURCES TABLE**
- **RESOURCE AVAILABILITY**
  - Lead contact
  - Materials availability
  - Data and code availability
- **EXPERIMENTAL MODEL AND SUBJECT DETAILS**
  - *Drosophila* stocks and maintenance
- **METHOD DETAILS**
  - Generation of transgenic *Drosophila* lines
  - *Drosophila* genetics
  - Antibodies and immunofluorescence
  - Quantitative RT-PCR
  - Fertility tests
- **QUANTIFICATION AND STATISTICAL ANALYSIS**
  - Data analysis and statistics

## SUPPLEMENTAL INFORMATION

Supplemental information can be found online at <https://doi.org/10.1016/j.devcel.2021.07.010>.

## ACKNOWLEDGMENTS

The authors thank members of the Bach lab, Jessica Treisman, Hyung Don Ryoo, Vilaiwan Fernandes, Will Wood, Arantza Barrios, and Richard Poole for discussions; Nazif Alic for help with statistics; and Aryeh Korman for help with imaging Babo-GFP.

For antibodies, the authors acknowledge the DHSB, created by the NICHD of the NIH and maintained at the University of Iowa, Department of Biology, Iowa City, IA 52242, and for plasmids, the authors acknowledge the DGRC at Indiana University, which is supported by a grant from the National Institutes of Health (ORIP and NIGMS). Work in the Bach lab is supported by grants from the NIH and New York State Department of Health/NYSTEM (C32584GG). Work in the Amoyel lab is supported by an Elizabeth Blackwell Institute Early Career Fellowship and an MRC Career Development award MR/P009646/2.

## AUTHOR CONTRIBUTIONS

Conceptualization, M.A. and E.A.B.; methodology, S.C.H., M.A., and E.A.B.; validation, M.A. and E.A.B.; formal analysis, S.C.H., M.A., and E.A.B.; investigation, S.C.H., M.A., D.S.d.I.M., L.G., S.M., R.P., and M.B.; resources, M.O., M.A., and E.A.B.; data curation, S.C.H., M.A., and E.A.B.; writing—original draft, S.C.H., M.A., and E.A.B.; writing—review and editing, S.C.H., M.A., and E.A.B.; visualization, S.C.H.; supervision, M.A. and E.A.B.; project administration, M.A. and E.A.B.; funding acquisition, M.A. and E.A.B.

## DECLARATION OF INTERESTS

The authors declare no competing interests.

## INCLUSION AND DIVERSITY

One or more of the authors of this paper self-identifies as an underrepresented ethnic minority in science.

One or more of the authors of this paper received support from a program designed to increase minority representation in science.

Received: January 22, 2021

Revised: May 14, 2021

Accepted: July 15, 2021

Published: August 6, 2021

## REFERENCES

- Amoyel, M., Sanny, J., Burel, M., and Bach, E.A. (2013). Hedgehog is required for CySC self-renewal but does not contribute to the GSC niche in the *Drosophila* testis. *Development* *140*, 56–65.
- Amoyel, M., Simons, B.D., and Bach, E.A. (2014). Neutral competition of stem cells is skewed by proliferative changes downstream of Hh and Hpo. *EMBO J* *33*, 2295–2313.
- Anllo, L., Plasschaert, L.W., Sui, J., and Dinardo, S. (2019). Live imaging reveals hub cell assembly and compaction dynamics during morphogenesis of the *Drosophila* testis niche. *Dev. Biol.* *446*, 102–118.
- Awasaki, T., Huang, Y., O'Connor, M.B., and Lee, T. (2011). Glia instruct developmental neuronal remodeling through TGF- $\beta$  signaling. *Nat. Neurosci.* *14*, 821–823.
- Bertet, C., Li, X., Erclik, T., Cavey, M., Wells, B., and Desplan, C. (2014). Temporal patterning of neuroblasts controls Notch-mediated cell survival through regulation of Hid or Reaper. *Cell* *158*, 1173–1186.
- Boyle, M., Wong, C., Rocha, M., and Jones, D.L. (2007). Decline in self-renewal factors contributes to aging of the stem cell niche in the *Drosophila* testis. *Cell Stem Cell* *1*, 470–478.
- Bragado, P., Estrada, Y., Parikh, F., Krause, S., Capobianco, C., Farina, H.G., Schewe, D.M., and Aguirre-Ghiso, J.A. (2013). TGF- $\beta$ 2 dictates disseminated tumour cell fate in target organs through TGF- $\beta$ -RIII and p38 $\alpha$ / $\beta$  signalling. *Nat. Cell Biol.* *15*, 1351–1361.
- Brummel, T., Abdollah, S., Haerry, T.E., Shimell, M.J., Merriam, J., Rafferty, L., Wrana, J.L., and O'Connor, M.B. (1999). The *Drosophila* activin receptor baboon signals through dSmad2 and controls cell proliferation but not patterning during larval development. *Genes Dev* *13*, 98–111.
- Chen, D., Pacal, M., Wenzel, P., Knoepfler, P.S., Leone, G., and Bremner, R. (2009). Division and apoptosis of E2F-deficient retinal progenitors. *Nature* *462*, 925–929.
- Diao, F., Ironfield, H., Luan, H., Diao, F., Shropshire, W.C., Ewer, J., Marr, E., Potter, C.J., Landgraf, M., and White, B.H. (2015). Plug-and-play genetic access to *Drosophila* cell types using exchangeable exon cassettes. *Cell Rep* *10*, 1410–1421.
- Dinardo, S., Okegbe, T., Wingert, L., Freilich, S., and Terry, N. (2011). Lines and bowl affect the specification of cyst stem cells and niche cells in the *Drosophila* testis. *Development* *138*, 1687–1696.
- Evans, C.J., Olson, J.M., Ngo, K.T., Kim, E., Lee, N.E., Kuoy, E., Patananan, A.N., Sitz, D., Tran, P., Do, M.-T., et al. (2009). G-TRACE: rapid Gal4-based cell lineage analysis in *Drosophila*. *Nat. Methods* *6*, 603–605.
- Fabrizio, J.J., Boyle, M., and Dinardo, S. (2003). A somatic role for eyes absent (*eya*) and sine oculis (*so*) in *Drosophila* spermatocyte development. *Dev. Biol.* *258*, 117–128.
- Fairchild, M.J., Yang, L., Goodwin, K., and Tanentzapf, G. (2016). Occluding junctions maintain stem cell niche homeostasis in the fly testes. *Curr. Biol.* *26*, 2492–2499.
- Flaherty, M.S., Salis, P., Evans, C.J., Ekas, L.A., Marouf, A., Zavadil, J., Banerjee, U., and Bach, E.A. (2010). chinmo is a functional effector of the JAK/STAT pathway that regulates eye development, tumor formation, and stem cell self-renewal in *Drosophila*. *Dev. Cell* *18*, 556–568.
- Forbes, A.J., Lin, H., Ingham, P.W., and Spradling, A.C. (1996). hedgehog is required for the proliferation and specification of ovarian somatic cells prior to egg chamber formation in *Drosophila*. *Development* *122*, 1125–1135.
- Fullerton, P.T., Jr., Monsivais, D., Kommagani, R., and Matzuk, M.M. (2017). Follistatin is critical for mouse uterine receptivity and decidualization. *Proc. Natl. Acad. Sci. USA* *114*, E4772–E4781.
- Ghajar, C.M., Peinado, H., Mori, H., Matei, I.R., Evason, K.J., Brazier, H., Almeida, D., Koller, A., Hajjar, K.A., Stainier, D.Y., et al. (2013). The perivascular niche regulates breast tumour dormancy. *Nat. Cell Biol.* *15*, 807–817.
- Greenspan, L.J., and Matunis, E.L. (2018). Retinoblastoma intrinsically regulates niche cell quiescence, identity, and niche number in the adult *Drosophila* Testis. *Cell Rep* *24*, 3466–3476.e8.

- Hétéi, P., De Cuevas, M., and Matunis, E. (2014). Conversion of quiescent niche cells to somatic stem cells causes ectopic niche formation in the *Drosophila* testis. *Cell Rep* 7, 715–721.
- Kitadate, Y., and Kobayashi, S. (2010). Notch and *egfr* signaling act antagonistically to regulate germ-line stem cell niche formation in *Drosophila* male embryonic gonads. *Proc. Natl. Acad. Sci. USA* 107, 14241–14246.
- Kurusu, M., Cording, A., Taniguchi, M., Menon, K., Suzuki, E., and Zinn, K. (2008). A screen of cell-surface molecules identifies leucine-rich repeat proteins as key mediators of synaptic target selection. *Neuron* 59, 972–985.
- Le Bras, S., and Van Doren, M. (2006). Development of the male germline stem cell niche in *Drosophila*. *Dev. Biol.* 294, 92–103.
- Leatherman, J.L., and Dinardo, S. (2008). *Zfh-1* controls somatic stem cell self-renewal in the *Drosophila* testis and nonautonomously influences germline stem cell self-renewal. *Cell Stem Cell* 3, 44–54.
- Lee, J.Y., Chen, J.Y., Shaw, J.L., and Chang, K.T. (2016). Maintenance of stem cell niche integrity by a novel activator of integrin signaling. *PLoS Genet* 12, e1006043.
- McGuire, S.E., Mao, Z., and Davis, R.L. (2004). Spatiotemporal gene expression targeting with the TARGET and gene-switch systems in *Drosophila*. *Sci. STKE* 2004, pl6.
- Michel, M., Kupinski, A.P., Raabe, I., and Bökel, C. (2012). Hh signalling is essential for somatic stem cell maintenance in the *Drosophila* testis niche. *Development* 139, 2663–2669.
- Morrison, S.J., and Spradling, A.C. (2008). Stem cells and niches: mechanisms that promote stem cell maintenance throughout life. *Cell* 132, 598–611.
- Oh, J., Lee, Y.D., and Wagers, A.J. (2014). Stem cell aging: mechanisms, regulators and therapeutic opportunities. *Nat. Med.* 20, 870–880.
- Okegbe, T.C., and Dinardo, S. (2011). The endoderm specifies the mesodermal niche for the germline in *Drosophila* via Delta-Notch signaling. *Development* 138, 1259–1267.
- Patel, P.H., Dutta, D., and Edgar, B.A. (2015). Niche appropriation by *Drosophila* intestinal stem cell tumours. *Nat. Cell Biol.* 17, 1182–1192.
- Pentek, J., Parker, L., Wu, A., and Arora, K. (2009). Follistatin preferentially antagonizes activin rather than BMP signaling in *Drosophila*. *Genesis* 47, 261–273.
- Peterson, A.J., and O'Connor, M.B. (2013). Activin receptor inhibition by *Smad2* regulates *Drosophila* wing disc patterning through BMP-response elements. *Development* 140, 649–659.
- Plaks, V., Kong, N., and Werb, Z. (2015). The cancer stem cell niche: how essential is the niche in regulating stemness of tumor cells? *Cell Stem Cell* 16, 225–238.
- Resende, L.P., Boyle, M., Tran, D., Fellner, T., and Jones, D.L. (2013). *Headcase* promotes cell survival and niche maintenance in the *Drosophila* testis. *PLoS One* 8, e68026.
- Sarov, M., Barz, C., Jambor, H., Hein, M.Y., Schmied, C., Suchold, D., Stender, B., Janosch, S., K J, V.V., Krishnan, R.T., et al. (2016). A genome-wide resource for the analysis of protein localisation in *Drosophila*. *eLife* 5, e12068.
- Schindelin, J., Arganda-Carreras, I., Frise, E., Kaynig, V., Longair, M., Pietzsch, T., Preibisch, S., Rueden, C., Saalfeld, S., Schmid, B., et al. (2012). Fiji: an open-source platform for biological-image analysis. *Nat. Methods* 9, 676–682.
- Song, W., Cheng, D., Hong, S., Sappe, B., Hu, Y., Wei, N., Zhu, C., O'Connor, M.B., Pissios, P., and Perrimon, N. (2017). Midgut-derived activin regulates glucagon-like action in the fat body and glycemic control. *Cell Metab* 25, 386–399.
- Song, X., Call, G.B., Kirilly, D., and Xie, T. (2007). Notch signaling controls germline stem cell niche formation in the *Drosophila* ovary. *Development* 134, 1071–1080.
- Sreejith, P., Jang, W., To, V., Hun Jo, Y., Biteau, B., and Kim, C. (2019). *Lin28* is a critical factor in the function and aging of *Drosophila* testis stem cell niche. *Aging (Albany, NY)* 11, 855–873.
- Terry, N.A., Tulina, N., Matunis, E., and Dinardo, S. (2006). Novel regulators revealed by profiling *Drosophila* testis stem cells within their niche. *Dev. Biol.* 294, 246–257.
- Toledano, H., D'Alterio, C., Czech, B., Levine, E., and Jones, D.L. (2012). The *let-7*-*Imp* axis regulates ageing of the *Drosophila* testis stem-cell niche. *Nature* 485, 605–610.
- Tsai, Y.C., and Sun, Y.H. (2004). Long-range effect of *upd*, a ligand for Jak/STAT pathway, on cell cycle in *Drosophila* eye development. *Genesis* 39, 141–153.
- Tulina, N., and Matunis, E. (2001). Control of stem cell self-renewal in *Drosophila* spermatogenesis by JAK-STAT signaling. *Science* 294, 2546–2549.
- Upadhyay, A., Moss-Taylor, L., Kim, M.J., Ghosh, A.C., and O'Connor, M.B. (2017). TGF- $\beta$  family signaling in *Drosophila*. *Cold Spring Harb. Perspect. Biol.* 9.
- Venken, K.J., Schulze, K.L., Haelterman, N.A., Pan, H., He, Y., Evans-Holm, M., Carlson, J.W., Levis, R.W., Spradling, A.C., Hoskins, R.A., and Bellen, H.J. (2011). MiMIC: a highly versatile transposon insertion resource for engineering *Drosophila melanogaster* genes. *Nat. Methods* 8, 737–743.
- Voog, J., Sandall, S.L., Hime, G.R., Resende, L.P., Loza-Coll, M., Aslanian, A., Yates, J.R., 3rd, Hunter, T., Fuller, M.T., and Jones, D.L. (2014). *Escargot* restricts niche cell to stem cell conversion in the *Drosophila* testis. *Cell Rep* 7, 722–734.
- Walkley, C.R., Shea, J.M., Sims, N.A., Purton, L.E., and Orkin, S.H. (2007). *Rb* regulates interactions between hematopoietic stem cells and their bone marrow microenvironment. *Cell* 129, 1081–1095.
- Wallenfang, M.R., Nayak, R., and Dinardo, S. (2006). Dynamics of the male germline stem cell population during aging of *Drosophila melanogaster*. *Aging Cell* 5, 297–304.
- Ward, E.J., Shcherbata, H.R., Reynolds, S.H., Fischer, K.A., Hatfield, S.D., and Ruohola-Baker, H. (2006). Stem cells signal to the niche through the Notch pathway in the *Drosophila* ovary. *Curr. Biol.* 16, 2352–2358.
- Xu, B., Feng, X., and Burdine, R.D. (2010). Categorical data analysis in experimental biology. *Dev. Biol.* 348, 3–11.
- Zappia, M.P., and Frolov, M.V. (2016). *E2F* function in muscle growth is necessary and sufficient for viability in *Drosophila*. *Nat. Commun.* 7, 10509.

## STAR★METHODS

### KEY RESOURCES TABLE

Reagent or Resource	SOURCE	IDENTIFIER
<b>Antibodies</b>		
Mouse monoclonal anti-Fasciclin III (Fas3) (1:50)	DSHB	Cat# 7G10 anti-Fasciclin III; RRID: AB_528238
Rabbit polyclonal anti-GFP (1:500)	Invitrogen	Cat# A-6455; RRID: AB_221570
Goat polyclonal anti-Vasa (1:200)	Santa Cruz	Cat# sc26877; RRID: AB_793877
Chicken polyclonal anti-GFP (1:500)	Abcam	Cat# ab13970; RRID: AB_300798
Rat monoclonal anti-N Cadherin (1:20)	DSHB	Cat# DN-ex #8; RRID: AB_528121
Rat monoclonal anti DE-Cadherin (1:20)	DSHB	Cat# DCad2; RRID: AB_528120
Mouse monoclonal anti-Eyes absent (Eya) (1:20)	DSHB	Cat# eya10H6; RRID: AB_528232
Rat monoclonal anti-Vasa	DSHB	Cat# anti-vasa; RRID: AB_760351
Mouse monoclonal anti- $\beta$ -galactosidase (1:500)	Promega	Cat# Z3781; RRID: AB_430877
Mouse monoclonal anti-Dp (1:5)	N. Dyson (MGH Charlestown, USA)	N/A
Rabbit polyclonal anti-Zfh1 (1:1000)	K. White (University of Chicago, USA)	N/A
Guinea pig polyclonal anti-Traffic jam (1:3000)	D. Godt (University of Toronto, Canada)	N/A
Cy3-AffiniPure Donkey Anti-Mouse IgG (1:400)	Jackson ImmunoResearch Labs	Cat# 715-165-150; RRID: AB_2340813
Alexa Fluor 488-AffiniPure Donkey Anti-Rabbit IgG (H+L) (1:400)	Jackson ImmunoResearch Labs	Cat# 711-545-152; RRID: AB_2313584
Cy3-AffiniPure Donkey Anti-Rabbit IgG (H+L)(1:400)	Jackson ImmunoResearch Labs	Cat# 711-165-152; RRID: AB_2307443
Cy5-AffiniPure Donkey Anti-Rabbit IgG (H+L) (1:400)	Jackson ImmunoResearch Labs	Cat# 711-175-152; RRID: AB_2340607
Alexa Fluor 488-AffiniPure Donkey Anti-Rat IgG (H+L) (1:400)	Jackson ImmunoResearch Labs	Cat# 712-545-150; RRID: AB_2340683
Cy3-AffiniPure Donkey Anti-Rat IgG (H+L) (1:400)	Jackson ImmunoResearch Labs	Cat# 712-165-150; RRID: AB_2340666
Cy5-AffiniPure Donkey Anti-Rat IgG (H+L) (1:400)	Jackson ImmunoResearch Labs	Cat# 712-175-150; RRID: AB_2340671
Alexa Fluor 488 AffiniPure Donkey Anti-Chicken IgY (IgG) (H+L) (1:400)	Jackson ImmunoResearch Labs	Cat# 703-545-155; RRID: AB_2340375
Cy3-AffiniPure Donkey Anti-Chicken IgY (IgG) (H+L) (1:400)	Jackson ImmunoResearch Labs	Cat# 703-165-155; RRID: AB_2340363
Cy5-AffiniPure Donkey Anti-Chicken IgY (IgG) (H+L) (1:400)	Jackson ImmunoResearch Labs	Cat# 703-175-155; RRID: AB_2340365
Cy3-AffiniPure Donkey Anti-Guinea Pig IgG (1:400)	Jackson ImmunoResearch Labs	Cat# 706-165-148; RRID: AB_2340460
Cy5-AffiniPure Donkey Anti-Guinea Pig IgG (H+L) (1:400)	Jackson ImmunoResearch Labs	Cat# 706-175-148; RRID: AB_2340462
Cy3-AffiniPure Donkey Anti-Goat IgG (H+L) (1:400)	Jackson ImmunoResearch Labs	Cat# 705-165-003; RRID: AB_2340411
Alexa Fluor 647 AffiniPure Donkey Anti-Goat IgG (H+L) (1:400)	Jackson ImmunoResearch Labs	Cat# 705-605-003; RRID: AB_2340436
<b>Chemicals, peptides, and recombinant proteins</b>		
VECTASHIELD Mounting Medium	Vector Laboratories	Cat# H-1000; RRID: AB_2336789
VECTASHIELD Mounting Medium with DAPI	Vector Laboratories	Cat# H-1200; RRID: AB_2336790
Paraformaldehyde, 16% w/v aq. soln., methanol free	Thermo Fisher Scientific	Cat# 43368-9L
TO-PRO-3 iodide (1 $\mu$ M)	Invitrogen	Cat# T3605
5-ethynyl-2'-deoxyuridine (EdU)	Invitrogen	Cat# A10044

(Continued on next page)

**Continued**

Reagent or Resource	SOURCE	IDENTIFIER
AF405 picolylazide	Click chemistry tools	Cat# 1308-5
Tris(3-Hydroxypropyl(triazolylmethyl)Amine	Sigma Aldrich	Cat# 762342
Sodium Ascorbate	Sigma Aldrich	Cat# PHR1279
Copper(II) sulfate	Fisher Scientific	Cat# 15617730
Molasses	LabScientific	Cat# FLY-8008-16
Agar	Mooragar	Cat# 41004
Cornmeal	LabScientific	Cat# FLY-8010-20
Yeast	LabScientific	Cat#FLY-8040-20F
Tegosept	Sigma	Cat# H3647-1KG
Reagent alcohol	Fisher	Cat# A962P4
Propionic acid	Fisher	Cat# A258500
<b>Experimental models: organisms/strains</b>		
<i>D. melanogaster</i> ; Oregon <sup>R</sup>	Bach lab	N/A
<i>D. melanogaster</i> ; P[GawB]NP1624/CyO (tj-GAL4)	Bach lab	Kyoto Stock Center: 104055 Flybase: FBst0302922
<i>D. melanogaster</i> ; nos-GAL4-VP16	Ruth Lehmann (Whitehead Institute, USA)	N/A
<i>D. melanogaster</i> ; C587-GAL4	Ruth Lehmann (Whitehead Institute, USA)	N/A
<i>D. melanogaster</i> ; fng-GAL4	Stephen Dinardo (Perelman School of Medicine, University of Pennsylvania, USA)	N/A
<i>D. melanogaster</i> ; eyaA3-GAL4 (denoted eya-GAL4)	Stephen Dinardo (Perelman School of Medicine, University of Pennsylvania, USA)	N/A
<i>D. melanogaster</i> ; upd-GAL4	Bach lab	N/A
<i>D. melanogaster</i> ; tub-GAL80 <sup>TS</sup>	Bloomington Drosophila stock Center (BDSC)	BDSC_7017 FlyBase: FBst0007017
<i>D. melanogaster</i> ; hh-LacZ	Bach lab	BDSC_5530 FlyBase: FBst0005530
<i>D. melanogaster</i> ; upd-LacZ	Bach lab	N/A
<i>D. melanogaster</i> ; hh-GAL80	This paper	N/A
<i>D. melanogaster</i> ; hh-QF	This paper	N/A
<i>D. melanogaster</i> ; w <sup>1118</sup> ; P[w[+mC]=UAS-lacZ.NZ]J312. Insertion on III	BDSC	BDSC_3956 FlyBase: FBst003956
<i>D. melanogaster</i> ; w <sup>1118</sup> ; P[w[+mC]=UAS-lacZ.NZ]20b. Insertion on II	BDSC	BDSC_3955 FlyBase: FBst003955
<i>D. melanogaster</i> ; UAS-GFP; Ubi-p63E(FRT.STOP)Stinger	BDSC	BDSC_32251
<i>D. melanogaster</i> ; w <sup>1118</sup> ; P[GD4444]v12722 (Dp-RNAi)	Vienna Drosophila Resource Center (VDRC)	VDRC_v12722 FlyBase: FBst0450633
<i>D. melanogaster</i> ; FRT <sup>42D</sup> , Dp <sup>a3</sup> /CyO	M. Frolov, University of Illinois at Chicago, USA	Flybase: FBgn0011763
<i>D. melanogaster</i> ; FRT <sup>42D</sup> , Dp <sup>a4</sup> /CyO	M. Frolov, University of Illinois at Chicago, USA	Flybase: FBgn0011763
<i>D. melanogaster</i> ; UAS-Dp	M. Frolov, University of Illinois at Chicago, USA	Flybase: FBgn0011763
<i>D. melanogaster</i> ; FRT <sup>82B</sup> E2f1 <sup>729</sup>	M. Frolov, University of Illinois at Chicago, USA	FlyBase: FBgn0011766
<i>D. melanogaster</i> ; y <sup>1</sup> , v <sup>1</sup> ; P[TRIP.JF02519] attP2/TM3, Sb <sup>1</sup> (Dp-RNAi)	BDSC	BDSC_30515 FlyBase: FBst0030515

(Continued on next page)

**Continued**

Reagent or Resource	SOURCE	IDENTIFIER
<i>D. melanogaster</i> ; <i>w</i> <sup>1118</sup> ; <i>P</i> [GD4448] <i>v15886</i> ( <i>E2f1-RNAi</i> )	VDRG	VDRG: v15886 FlyBase: FBst0452055
<i>D. melanogaster</i> ; <i>UAS-Rbf</i> <sup>280</sup> Insertion on III	W. Deng (Tulane University, USA)	BDSC_50748 Flybase: FBst0050748
<i>D. melanogaster</i> ; <i>act&gt;y[+]&gt;LHV2-86Fb,13XlexAop2-myr::GFP</i> ( <i>FLEX-AMP</i> )	C. Desplan (New York University, USA)	N/A
<i>D. melanogaster</i> ; <i>UAS-FLP</i>	BDSC	BDSC_4539
<i>D. melanogaster</i> ; <i>QUAS-FLP</i>	BDSC	BDSC_30126
<i>D. melanogaster</i> ; <i>w</i> <sup>1118</sup> ; <i>P</i> [GD15843] <i>v46260</i> ( <i>Fs-RNAi</i> )	VDRG	VDRG v46260 FlyBase: FBst0466595
<i>D. melanogaster</i> ; <i>y</i> <sup>1</sup> <i>v</i> <sup>1</sup> ; <i>P</i> [TRiP.HMJ03135] <i>attP40</i> ( <i>daw-RNAi</i> )	BDSC	BDSC_50911 Flybase: FBst0050911
<i>D. melanogaster</i> ; <i>P</i> [KK110248] <i>VIE-260B</i> ( <i>daw-RNAi</i> )	VDRG	VDRG #v105309 Flybase: FBst0477137
<i>D. melanogaster</i> ; <i>y</i> <sup>1</sup> <i>sc</i> * <i>v</i> <sup>1</sup> <i>sev</i> <sup>21</sup> ; <i>P</i> [TRiP.HMS01110] <i>attP2</i> ( <i>daw-RNAi</i> )	BDSC	BDSC_34974 Flybase: FBst0034974
<i>D. melanogaster</i> ; <i>y</i> <sup>1</sup> <i>v</i> <sup>1</sup> ; <i>P</i> [TRiP.GL01476] <i>attP2</i> ( <i>smox-RNAi</i> )	BDSC	BDSC_43138 Flybase: FBst0043138
<i>D. melanogaster</i> ; <i>y</i> <sup>1</sup> <i>w</i> <sup>*</sup> ; <i>Mi</i> [MIC] <i>Fs</i> <sup>Mi01433</sup> ( <i>Fs</i> <sup>Mi01433</sup> )	BDSC	BDSC_33121 Flybase: FBst0033121
<i>D. melanogaster</i> ; <i>y</i> <sup>1</sup> <i>w</i> <sup>*</sup> ; <i>Mi</i> [MIC] <i>Fs</i> <sup>Mi11350</sup> ( <i>Fs</i> <sup>Mi11350</sup> )	BDSC	BDSC_56310 Flybase: FBst0056310
<i>D. melanogaster</i> ; <i>y</i> <sup>1</sup> <i>w</i> <sup>*</sup> ; <i>Fs</i> <sup>Mi04308-TG4.1</sup> <i>CG8079</i> <sup>Mi04308-TG4.1-X</sup> ( <i>Fs</i> <sup>TJ4.1</sup> )	BDSC	BDSC_66838 (lost during the pandemic)
<i>D. melanogaster</i> ; <i>y</i> <sup>1</sup> <i>w</i> <sup>*</sup> ; <i>Mi</i> [PT-GFSTF.1] <i>Fs</i> <sup>Mi04308-GFSTF.1</sup> <i>CG8079</i> <sup>Mi04308-GFSTF.1-X</sup> <i>/CyO</i> ( <i>Fs</i> <sup>GFSTF.1</sup> or <i>Fs-GFP</i> )	BDSC	BDSC_65327 Flybase: FBst0065327
<i>D. melanogaster</i> ; <i>Fs</i> <sup>null</sup>	This paper	N/A
<i>D. melanogaster</i> ; <i>UAS-Fs</i>	O'Connor lab	N/A
<i>D. melanogaster</i> ; <i>Fs-GAL4</i> ( <i>Fs</i> <sup>Mi</sup> - <i>GAL4</i> )	This paper	N/A
<i>D. melanogaster</i> ; <i>UAS-esgNLAP</i>	L. Jones (UCSF, USA)	N/A
<i>D. melanogaster</i> ; <i>UAS-NLAP</i>	L. Jones (UCSF, USA)	N/A
<i>D. melanogaster</i> ; <i>Actβ-GAL4</i>	O'Connor lab	N/A
<i>D. melanogaster</i> ; <i>myo-GAL4</i>	O'Connor lab	N/A
<i>D. melanogaster</i> ; <i>y</i> <sup>1</sup> <i>w</i> <sup>*</sup> ; <i>Mi</i> [MIC] <i>daw</i> <sup>Mi05383</sup> ( <i>daw-GFP</i> )	BDSC	BDSC_43001 Flybase: FBst0043001
<i>D. melanogaster</i> ; <i>UAS-babo-RNAi</i> .	O'Connor lab	N/A
<i>D. melanogaster</i> ; <i>UAS-babo</i> <sup>QD</sup>	O'Connor lab	N/A
<i>D. melanogaster</i> ; <i>PBac</i> [fTRG00506. <i>sfGFP-TVPTBF</i> ] <i>VK00033</i> ( <i>Actβ</i> <sup>fTRG00506.sfGFP-TVPTBF</sup> )	VDRG	VDRG #v318136 Flybase: FBst0491562
<i>D. melanogaster</i> ; <i>PBac</i> [fTRG00161. <i>sfGFP-TVPTBF</i> ] <i>VK00033</i> ( <i>myo</i> <sup>fTRG00161.sfGFP-TVPTBF</sup> )	VDRG	VDRG #v318065 Flybase: FBst0491390
<i>D. melanogaster</i> ; <i>PBac</i> [fTRG00444. <i>sfGFP-TVPTBF</i> ] <i>VK00033</i> ( <i>babo</i> <sup>fTRG00444.sfGFP-TVPTBF</sup> )	VDRG	VDRG #v318433 Flybase: FBst0491516
<i>D. melanogaster</i> ; <i>w</i> <sup>*</sup> ; <i>P</i> [GawB] <i>daw</i> <sup>NP4661</sup> / <i>CyO</i> ( <i>daw</i> <sup>NP4661</sup> - <i>GAL4</i> )	Kyoto Stock Center	Kyoto #113490 Flybase: FBst0316217
<i>D. melanogaster</i> ; <i>y</i> <sup>*</sup> <i>w</i> <sup>*</sup> ; <i>P</i> [GawB] <i>daw</i> <sup>NP6274</sup> / <i>CyO</i> ( <i>daw</i> <sup>NP6274</sup> - <i>GAL4</i> )	Kyoto Stock Center	Kyoto #105179 Flybase: FBst0304038

(Continued on next page)

### Continued

Reagent or Resource	SOURCE	IDENTIFIER
<b>Oligonucleotides</b>		
gRNA Fs 1	5' CCGGTTGCATCATGTATCTTGGC 3'	IDTDNA
gRNA Fs 2	5' CCAACTGGAGGTCGCCTATCGGG 3'	IDTDNA
qPCR primer <i>Fs</i> -fwd:	5'-AGTGTCATATATACTCTCCGCATGT-3'	IDTDNA
qPCR primer <i>Fs</i> -rev:	5'-ACAGCAACTGCTTTTAACTATGCC-3'	IDTDNA
qPCR primer $\alpha$ - <i>tub84B</i> -fwd:	5'-TCGTTTTACGTTTGTC AAGCCTC-3'	IDTDNA
qPCR primer $\alpha$ - <i>tub84B</i> -rev:	5'-GAGATACATTCACGCATATTGAGTT-3'	IDTDNA
qPCR primer <i>daw</i> -fwd	5'-CCCATCTTCGACGGGATGAC-3'	IDTDNA
qPCR primer <i>daw</i> -rev	5'-TTGCACTCGACCTCCTCTCT-3'	IDTDNA
<b>Software and algorithms</b>		
ImageJ/Fiji	Fiji	<a href="http://fiji.sc/">http://fiji.sc/</a>
Photoshop/Illustrator	Adobe	<a href="https://www.adobe.com/products/">https://www.adobe.com/products/</a>
Prism	GraphPad	<a href="https://www.graphpad.com">https://www.graphpad.com</a>
ZEN	Zeiss	<a href="https://www.zeiss.com/microscopy/us/products/microscope-software/zen.html">https://www.zeiss.com/microscopy/us/products/microscope-software/zen.html</a>
Excel	Microsoft	<a href="https://products.office.com/en-us/excel">https://products.office.com/en-us/excel</a>
Imaris	Oxford Instruments	<a href="https://imaris.oxinst.com/">https://imaris.oxinst.com/</a>

## RESOURCE AVAILABILITY

### Lead contact

Further information and requests for resources and reagents should be directed to and will be fulfilled by the Lead Contact, Erika Bach ([erika.bach@nyu.edu](mailto:erika.bach@nyu.edu)).

### Materials availability

All *Drosophila* stocks generated in this study are available from the Lead Contact without restriction.

### Data and code availability

- All data reported in this paper will be shared by the Lead Contact upon request.
- This paper does not report original code
- Any additional information required to reanalyze the data reported in this paper is available from the lead contact upon request

## EXPERIMENTAL MODEL AND SUBJECT DETAILS

### *Drosophila* stocks and maintenance

*Drosophila melanogaster* strains used in this study are listed in the [key resources table](#). *Drosophila* were reared on food made with these ingredients: 1800mL molasses (LabScientific, Catalog no. FLY-8008-16), 266 g agar (Mooragar, Catalog no. 41004), 1800 g cornmeal (LabScientific, Catalog no. FLY-8010-20), 744g Yeast (LabScientific, Catalog no. FLY-8040-20F), 47 L water, 56 g Tego-sept (Sigma no. H3647-1KG), 560mL reagent alcohol (Fisher no. A962P4), and 190mL propionic acid (Fisher no. A258500).

Flies were kept at 25°C, except crosses with *GAL80<sup>TS</sup>*, which were maintained at 18°C until eclosion, and the adult flies were transferred to 29°C. Clonal experiments were analyzed at 2 dpcl to assess clone induction and 7 and 14 dpcl for maintenance as is standard in the field (Amoyel et al., 2014). For transgene expression in CySCs, we examined hub cell number at 0, 3, 7, 10 and 20 days of adulthood. Our reason for selecting these time points is that Dp knockdown by *tj-GAL4* led to an almost complete loss of hub cells by 10 days, but since other genotypes exhibited a slower loss of hub cells, we also examined hub cells at 20 days of adulthood. We looked at earlier time points (3 and 7 days) to examine hubs before their complete loss. For the aging experiments, we examined hub cell number at 1, 2, 3, or 4 weeks (or 7, 14, 21, 28 days) of adulthood.

Males were aged separately from females and provided with fresh food every other day. For adult-onset overexpression and RNAi-depletion, we used the appropriate driver combined with the temperature-sensitive repressor *tub-GAL80<sup>TS</sup>*. Flies were reared at the permissive temperature (18°C) and adult males were collected and shifted to the restrictive temperature of 29°C to allow GAL4 activity. Experiments without GAL80 were raised at room temperature until eclosion and shifted to 29°C for the specified period to ensure maximum GAL4 activity.

We used the following fly stocks: *Oregon-R*; *tj-GAL4* (Kyoto Stock Center #NP1624); *nos-GAL4-VP16* (gift of Ruth Lehmann, Whitehead Institute, USA); *upd-LacZ* (Tsai and Sun, 2004); *hh-LacZ*; *tub-GAL80<sup>TS</sup>* (McGuire et al., 2004); *hh-GAL80* (this study); *hh-QF* (this study); *UAS-LacZ* (Bloomington Drosophila Stock center (BDSC) #3955 and 3956); *UAS-GFP*; *Ubi-p63E(FRT.STOP)Stinger* (also known as GTRACE, BDSC # 32251); *UAS-Dp RNAi* (Vienna Drosophila Resource Center (VDRC) #v12722); *FRT<sup>42D</sup>Dp<sup>a3</sup>* and *FRT<sup>42D</sup>Dp<sup>a4</sup>* (both gifts of M. Frolov, University of Illinois at Chicago, USA); *FRT<sup>92B</sup>E2f1<sup>729</sup>* (gift of M. Frolov); *UAS-Dp RNAi* (BDSC #30515); *UAS-Dp* (Zappia and Frolov, 2016) (gift of M. Frolov); *UAS-E2f1 RNAi* (VDRC #v15886); *UAS-Rbf<sup>280</sup>* (BDSC #50748); *act>y[+]>LHV2-86Fb,13XlexAop2-myr::GFP* (also known as FLEXAMP (Bertet et al., 2014)) where *LHV2-86Fb* encodes an optimized version of LEXA-VP16 with reduced toxicity; *UAS-FLP* (BDSC #4539); *QUAS-FLP* (BDSC #30126); *UAS-Fs-RNAi* (*GD15843*, VDRC #v46260); *UAS-daw-RNAi* (*HMJ03135* BDSC #50911; *HMS01110* BDSC #34974; and *KK110248* VDRC #v105309); *UAS-smox-RNAi* (*GL01476* BDSC #43138); *Fs<sup>M101433</sup>* (BDSC #33121); *Fs<sup>M11350</sup>* (BDSC #56310); *Fs<sup>M104308-TG4.1</sup>* *CG8079<sup>M104308-TG4.1-X</sup>* (referred to as *Fs<sup>TJ4.1</sup>*, BDSC #66838); *Fs<sup>M104308-GFSTF.1</sup>* *CG8079<sup>M104308-GFSTF.1-X</sup>* (referred to as *Fs<sup>GFSTF.1</sup>* or *Fs-GFP*) BDSC #65327); *Fs<sup>null</sup>* (this study); *UAS-Fs* (Pentek et al., 2009); *Fs-GAL4* (referred to also as *Fs<sup>M1</sup>-GAL4*) (this study); *UAS-esgNLAP* and *UAS-NLAP* (both gifts from Leanne Jones, UCLA, USA) (Voog et al., 2014); *Actβ-GAL4* (Song et al., 2017); *myo-GAL4* (Awasaki et al., 2011); *daw<sup>M105383</sup>* (referred to as *daw-GFP*, BDSC #43001); *UAS-babo-RNAi* (Peterson and O'Connor, 2013); *UAS-babo<sup>QD</sup>*; *Actβ<sup>TTRG00506.sfGFP-TVPTBF</sup>* (Sarav et al., 2016), VDRC #v318136); *myo<sup>TTRG00161.sfGFP-TVPTBF</sup>* (Sarav et al., 2016), VDRC #v318065); *babo<sup>TTRG00444.sfGFP-TVPTBF</sup>* (Sarav et al., 2016), VDRC #v318433); *punt* (*put*)<sup>TTRG00910.sfGFP-TVPTBF</sup> (Sarav et al., 2016), VDRC #v318264); *daw<sup>NP4661</sup>-GAL4* and *daw<sup>NP6274</sup>-GAL4*, *UAS-LacZ* (Kyoto Stock Center #113490 and #105179, respectively).

## METHOD DETAILS

### Generation of transgenic *Drosophila* lines

The *Fs-GAL4* line used to monitor *Fs* transcriptional activity was created by recombination mediated cassette exchange (RMCE) to insert *GAL4* in the MiMIC line *Fs<sup>M101433</sup>* (Venken et al., 2011). The *Fs<sup>null</sup>* mutant was created by GenetiVision using CRISPR/Cas9 to delete 3 kb of the *Fs* locus, corresponding to the first 4 coding exons of both predicted *Fs* isoforms (Figure S3D). This genomic region was replaced by a splicing acceptor site and stop codons in all the 3 frames, followed by a 3xP3-GFP cassette. We used CCGGTTGCATCATGTATCTTGGC and CCAACTGGAGGTCGCCTATCGGG as gRNAs. We validated the mutant by sequencing the PCR product using the genomic DNA from the *Fs<sup>null</sup>* mutant as a template and the following primers:

fwd 5' CGGTGCATAATGCGCCAAACC 3'  
rev 5' CTTGCAGTGCACCTGGATATGG 3'

*hh-GAL80* and *hh-QF* were generated by RMCE by injection into line *M110526* (BDSC #53865), carrying a MiMIC transposon in the *hh* locus, using plasmids from the *Drosophila* Genomics Resource Center (DGRC) #1390 (Diao et al., 2015) and #1296 (Venken et al., 2011), respectively.

### *Drosophila* genetics

To label the lineage of hub cells, we used *upd-GAL4* and *tub-GAL80<sup>TS</sup>* to drive expression of the *UAS-FLP* recombinase, which excises a stop from the *ubiP63E(FRT.STOP)Stinger* G-TRACE cassette (Evans et al., 2009). After the excision of FRT sites following recombination, the resulting GFP serves an indelible and persistent marker to identify CySCs derived from the hub lineage. For tracing the hub lineage while manipulating expression in the cyst lineage, we used *C587-GAL4* to knock down *Dp* in CySCs, and an orthogonal expression system, *hh-QF*, to drive *QUAS-FLP* expression in hub cells. The lineage was permanently marked upon FLP expression using either the GTRACE cassette, as above, or the FLEXAMP cassette, in which a *yellow<sup>+</sup>* transgene is excised by FLP, leading to permanent expression of LexA under the *actin* promoter. LexA labels cells through expression of *myr-GFP*, driven by multimerized *LexAop* binding sites.

For mutant clones, crosses were raised at 25°C until eclosion. Males were collected for up to 2 days, then heat-shocked at 37°C for 1 h and returned to 25°C until dissection, 2, 7 or 14 days later.

### Antibodies and immunofluorescence

The following primary antibodies were used: goat anti-Vasa (1:200; Santa Cruz), mouse anti-Fasciclin3 (Fas3) (1:50; Developmental Studies Hybridoma Bank (DSHB), mouse anti-Eya (1:20, DSHB), rat anti-Vasa (1:20, DSHB), rat anti-N-Cadherin (1:20, DSHB), rabbit anti-GFP (1:500; Invitrogen), chicken anti-GFP (1:500, Aves Labs), mouse anti-β-Galactosidase (1:500, Promega), guinea pig anti-Tj (1:3000, a gift of Dorothea Godt, University of Toronto, Canada), rabbit anti-Zfh1 (1:1000), mouse anti-Dp (1:5, a gift of Nick Dyson, MGH Charlestown, USA), TO-PRO-3 iodide (1 μM; Molecular Probes); 4',6-diamidino-2-phenylindole (DAPI) (1:500, Invitrogen). Donkey secondary antisera were used 1:400 (Jackson ImmunoResearch). Dissections and staining were carried out as previously described (Flaherty et al., 2010). In brief, testes were dissected in 1x phosphate buffered saline (PBS), fixed for 15 min in 4% formaldehyde in 1xPBS, washed for 1 h at 25°C in 1xPBS with 0.5% Triton X-100, and blocked in PBTB (1xPBS 0.2% Triton X-100 and 1% bovine serum albumin) for 1 h at 25°C. Primary antibodies were incubated overnight at 4°C. They were washed two times for 30 min in PBTB and incubated 2 h in secondary antibody in PBTB at 25°C and then washed two times for 30 min in 1x PBS with 0.2% Triton X-100. They were mounted in Vectashield or Vectashield + DAPI (Vector Laboratories). 5-ethynyl-2'-deoxyuridine (EdU) labeling was achieved by incubating dissected samples in 10 μM EdU (Life Technologies) in Schneider's medium prior to fixation. Following

primary and secondary antibody incubations and washes, samples were incubated for 30 min in buffer containing 0.1M THPTA, 2mM sodium ascorbate, 1mM CuSO<sub>4</sub> and 2.5μM picolylazide conjugated to a fluorophore (Alexa 405, 488, 568 or 643, Click Chemistry Tools). Samples were then washed and mounted for imaging. Confocal images were captured using Zeiss LSM 510, LSM 700, LSM 880 and a Leica Sp8confocal microscopes with a 63x objective.

### Quantitative RT-PCR

Whole testes (n=20-25) were isolated and mRNA was extracted with PicoPure RNA Isolation system (Applied Biosystems) following the manufacturer's instructions. Reverse transcription was performed using Maxima Reverse Transcriptase (ThermoFisher) as per manufacturer's instructions and using 0.5μg of RNA as template. qRT-PCR was performed using SYBR Green PCR Master Mix (ThermoFisher) and a QuantStudio 5 Real-Time PCR System machine (Applied Biosystems). 8 replicates were performed for the experiments in [Figures 5H](#) and [4](#) replicates for each experiment shown in [Figure S3E](#). To detect *Fs* isoform B (FlyBase code FBtr0339996), we used the following primers and normalized expression levels to the control gene *α-tub84B*:

*Fs*-fwd: 5'-AGTGTCATATATACTCTCCGCATGT-3'

*Fs*-rev: 5'-ACAGCAACTGCTTTTAACTATGCC-3'

*α-tub84B*-fwd: 5'-TCGTTTTACGTTTGTCAAGCCTC-3'

*α-tub84B*-rev: 5'-GAGATACATTCACGCATATTGAGTT-3'

*daw*-fwd: 5'-CCCATCTTCGACGGGATGAC-3'

*daw*-rev: 5'-TTGCACTCGACCTCCTCTCT-3'

We failed to detect transcripts of *Fs* isoform A in the testis (FlyBase FBtr0087398), using the following primers and normalized expression levels to the control gene *α-tub84B*:

*Fs*-A-fwd: 5'-GAACGGACCGCGCTAAAAAT-3'

*Fs*-A-rev: 5'-GGCAAACGCACTGGTTTCAT-3'

### Fertility tests

Mutant males were crossed individually with two *Oregon<sup>R</sup>* females. After 48 h of mating and egg laying, all adults were removed from the vials. The size of the brood of each male was scored ten days later.

## QUANTIFICATION AND STATISTICAL ANALYSIS

### Data analysis and statistics

Hub cells were quantified by counting nuclei (labelled with DAPI, or low levels of Tj or Zfh1) in cells that were also Fas3-positive.

For GFP intensity quantifications, we dissected control flies and experiments on the same day and processed them simultaneously. Images were acquired with the same microscope settings. Plots show mean fluorescence intensity normalized to the average value of the controls.

The percentage of transdifferentiated CySCs was calculated as the ratio of Zfh1-positive cells simultaneously positive for the hub cell-lineage labeling.

Image processing, quantifications, and figure preparation were performed with Fiji-ImageJ ([Schindelin et al., 2012](#)), Adobe Photoshop and Adobe Illustrator software. Statistical tests were performed using GraphPad Prism8 or JMP software. To test for an interaction between genotype and aging in [Figures 5D](#) and [5E](#), we used a linear model featuring full factorial design and tested for the effect of both age and genotype on hub cell number and their interaction. Categorical data analysis in [Figures 4D](#) and [S1B](#), [S1G](#), and [S5B](#) was performed as described in ([Xu et al., 2010](#)) using Fisher's Exact tests. Other data were analyzed with Student's t tests because they were pairwise comparisons between genotypes. Data were analyzed and plotted with GraphPad Prism8. In all graphs, whiskers indicate the entire range of data, the boxes show the second and third quartiles and the line shows the median.